

Article

# Application of Transient Analysis Techniques to Fault Diagnosis in Low- and Medium-Power Synchronous Machines

Angela Navarro-Navarro <sup>1</sup>, Jose E. Ruiz-Sarrio <sup>1</sup>, Vicente Biot-Monterde <sup>1</sup>, Jose A. Antonino-Daviu <sup>1,\*</sup>, Vincent Becker <sup>1,2</sup> and Sven Urschel <sup>2</sup>

<sup>1</sup> Instituto Tecnológico de la Energía (ITE), Universitat Politècnica de València (UPV), Camino de Vera S/N, 46022 Valencia, Spain

<sup>2</sup> Department of Engineering, University of Applied Sciences Kaiserslautern, Schoenstraße 11, 67659 Kaiserslautern, Germany

\* Correspondence: joanda@die.upv.es

**Abstract:** Fault diagnosis techniques applied to synchronous motors such as Permanent Magnet Synchronous Machines (PMSMs) and Synchronous Reluctance Machines (SynRMs) are scarcely addressed in the literature, in strong contrast to the attention paid to asynchronous motors. In addition, the most widespread techniques are those based on steady-state condition analysis, and little attention is paid to detection during transient operation. The present paper aims to identify research gaps on the topic and to demonstrate the potential of transient analysis. First, the different diagnostic methodologies in literature are thoroughly analyzed. Then, two laboratory case studies are presented to demonstrate the potential of fault detection under non-stationary conditions for a PMSM and a SynRM. Stator current analysis is performed by building time–frequency maps to analyze the evolution of different fault indicators. The results show clear differences between healthy and faulty conditions during the transient regime.

**Keywords:** synchronous motors; fault diagnosis; transient analysis; permanent magnet machines; synchronous reluctance machine; maintenance; misalignment; eccentricity; unbalance



**Citation:** Navarro-Navarro, A.; Ruiz-Sarrio, J.E.; Biot-Monterde, V.; Antonino-Daviu, J.A.; Becker, V.; Urschel, S. Application of Transient Analysis Techniques to Fault Diagnosis in Low- and Medium-Power Synchronous Machines. *Machines* **2023**, *11*, 288. <https://doi.org/10.3390/machines11020288>

Academic Editor: Ahmed Abu-Siada

Received: 29 December 2022

Revised: 10 February 2023

Accepted: 12 February 2023

Published: 14 February 2023



**Copyright:** © 2023 by the authors. Licensee MDPI, Basel, Switzerland. This article is an open access article distributed under the terms and conditions of the Creative Commons Attribution (CC BY) license (<https://creativecommons.org/licenses/by/4.0/>).

## 1. Introduction

Rotating electrical machines are extensively utilized in key sectors such as transportation and industry. Moreover, the utilization of such technology for energy conversion represents an important fraction of worldwide energy consumption [1]. Nowadays, the trend towards a more electrified world accentuates the role of electrical generators and actuators [2]. High-power energy generation traditionally included large rotating machines, and only in recent times have electrical motors become the preferred choice for several low- and medium-power applications such as automotive traction. The usage of the induction motor in low- and medium-power applications prevails due to its robustness, universal availability, and the capacity to work without further regulation except the supply at grid frequency. However, this does not represent the best alternative in all motoring scenarios (e.g., high torque density necessities, increased accuracy for speed and torque control, etc.). The more common availability of variable-frequency drives and the need for motor alternatives gave rise to the usage of synchronous machines in low- and medium-power applications such as fluid pumping, forced convection, transportation traction, etc. In particular, Permanent Magnet Synchronous Machines (PMSMs) are commonly utilized for high power density applications [3]. These machines utilize rare earth magnets, which are allocated in the rotor and create a constant magnetic flux rotating in a synchronous mode with the stator field. The magnets represent the main drawback of such machines, since they are a strategic resource, and their associated cost is normally high. Alternatives such as Synchronous Reluctance Machines (SynRM) or Permanent Magnet Assisted Synchronous

Reluctance Machines (PMASynRM) represent a feasible solution to the rare earth problem, and they have attracted research attention in recent years [4,5].

Rotating machines such as PMSMs, SynRMs and PMASynRMs are robust but not immune to wear and degradation of their different constructive elements. The proper maintenance of the motors is primordial when they constitute the core of critical applications, such as transportation and energy generation. A wide number of techniques are found for rotating machinery fault diagnosis and condition monitoring, where signals of various nature are analyzed offline or online [6]. The main drawback of offline methods is the need for the machine to be disconnected and disassembled to diagnose its status, which implies additional costs for the user due to the need for scheduled maintenance and production downtimes. Online methods offer the possibility of continuous motorization of the machine status, which enables the utilization of condition-based maintenance of the motor. This represents an advantage in terms of resources and costs across the machine lifecycle, since maintenance of the motor is required only when a faulty scenario occurs or is about to happen. Therefore, online monitoring and predictive maintenance for rotating electrical machines represent a broad area of study within the electrical machines and drives field.

The current trend for rotating machine condition monitoring and predictive maintenance is moving towards the development of smart systems where signals of different natures are synthesized and processed. Analyzed signals for online monitoring can be electrical (i.e., current and voltage), thermal, mechanical (i.e., vibrations), or magnetic (i.e., air-gap and stray magnetic flux). No method dependent on a single quantity is yet able to provide a fully reliable diagnostic of the machine, which makes the combination of different signals necessary to achieve proper diagnosis. In addition, well-established techniques such as the Motor Current Signature Analysis (MSCA) can provide false indicators under specific scenarios (e.g., load torque oscillations, machines with rotor axial cooling ducts, varying operating conditions, etc.) [7,8]. Thus, new techniques for reliable diagnosis such as sensor fusion [9] and transient signal analysis [10] arise to provide solutions to traditional detection issues.

The study of different signals during transient machine operation provides a valid solution to some of the traditional constraints. The main asset of these transient analysis techniques is the ability to detect faults through all the operational states of the machine (i.e., both steady-state and transient operation). Therefore, they are of capital importance in applications with repeated variation of the operating speed and torque profile, such as automotive traction, directly coupled wind generation, etc. In addition, they provide valuable information to discriminate between different types of faults, which are subjected to false diagnosis when studied during steady-state regimes [11]. The vast majority of works in the area of fault diagnosis under transient operation are applied to induction motors. Many works such as [8,9] study the current signature during the machine start-up. Moreover, vibration and stray flux signals are also utilized during the transient operation of induction machines, as observed in [12,13]. The major drawback of transient analysis tools is the need for more sophisticated signal processing tools working in the time–frequency domain. These are normally more computationally exigent than traditional steady-state focused applications such as the Fast Fourier Transform (FFT).

For novel motoring scenarios when the induction machine does not represent the best alternative, a lack of diagnostic methodologies in the literature is observed. In particular, techniques focused on diagnosis during transient operation are scarce, representing a research gap in the field. The present work is oriented towards the review and discussion of diagnostic methodologies applied to PMSMs, PMASynRMs, and SynRMs. These motors are normally utilized in low- and medium-power applications when increased efficiency and power density are pursued. Section 2 presents a thorough literature review where different methods are described and classified for different synchronous motor faults. Moreover, Section 3 describes two original laboratory cases, where eccentricity and misalignment faults during a transient regime are discussed for a PMSM and a SynRM respectively. Section 4 shows the main conclusions of the study and future research directions in the field.

## 2. Fault Detection

### 2.1. Stator Winding Short Circuits

Electrical defects in the stator winding are among the main causes of AC machine faults, accounting for 36% of failures in low-voltage applications [14]. These faults start with an inter-turn short-circuit (ITSC) within a coil. The initial ITSC is caused by an insulation defect derived from mechanical or electrical stresses, overheating, abrasion, etc. ITSCs can quickly develop into critical types of short-circuit such as coil-to-coil, phase-to-phase, and coil-to-ground. Therefore, it is important to detect ITSCs early on their development phase to avoid further damage to the insulation and conductors. Stator winding short circuits are particularly dangerous for PMSMs since they can cause partial or global demagnetization of the rotor magnets [15].

The most widespread techniques for ITSC detection are frequency-domain methods such as FFT analysis. Short circuits generate negative sequence currents [16], so techniques based on steady-state current analysis are widely used. The application of this technique consists of monitoring stator current and subsequent FFT analysis to obtain the amplitude of characteristic frequencies of the failure. The characteristic components for ITSC are calculated as follows [17]:

$$f_{ITSC} = f_s \left( 1 \pm \frac{k}{p} \right) \quad (1)$$

where  $f_s$  is the supply frequency,  $k$  is the positive integer, and  $p$  is the number of pole pairs.

According to [18–21], FFT analysis of the current shows an increase in the amplitude of the  $3f_s$  component. This is confirmed by other current-based techniques such as bi-spectrum (BS), power spectrum density (PSD), and MUSIC [22]. However, many of the studies reveal an increase in the  $2f_s$  component instead of the  $3f_s$  component when an ITSC exists [23]. In addition to steady-state FFT current analysis, the study of stator currents can be addressed by analyzing the current envelope [20,24] and the current negative sequence component [25]. Voltage signals are studied in [26] where FFT and PCA analysis are applied to extract fault indicators. The conclusion of this study is that the eigenvalues of the line-to-line voltage components are an indicator of ITSC faults. Furthermore, the first 14th harmonic of the voltage can be utilized as an ITSC fault indicator, according to [17]. The zero-sequence voltage component (ZSVC) and voltage in the  $dq$  reference frame are studied in [27,28], respectively. However, these techniques require access to a reference point. In [29] the speed is analyzed to detect short-circuit faults.

Transient analysis in PMSM for ITSC faults is quite widespread. The most commonly used diagnostic signal is the stator current. The Short-Time Fourier Transform (STFT) is utilized to detect ITSC faults in [30], where the Root Mean Square (RMS) value of the local maximum is used as a fault indicator. The advantage of this technique lies in its good performance when changes in speed or torque exist. The main drawback is the difficulty of compromise between frequency and time resolutions. The Hilbert–Huang Transform (HHT) is a fairly widely used technique in transient analysis [31,32]. Its main disadvantage lies in the difficulty of detecting the failure in the initial stages, which is a key necessity for ITSC diagnosis. The q-axis current is studied in [33,34], where the STFT is applied. This technique is also applied to the ZSVC in [27], where an increase in power frequency is utilized as an indicator of failure. Discrete signal processing techniques such as the Discrete Wavelet Transform (DWT) are applied to both the ZSVC [35,36] and q-axis voltage [37]. However, they present similar disadvantages when compared with continuous time–frequency transforms.

Despite the growing interest in synchronous reluctance motors, studies on ITSC detection for this type of motor are quite scarce. In [38], the authors propose a model of the machine where, the odd triple-order harmonics of the supply frequency are accentuated when a phase-to-phase short circuit is emulated. A recent work analyzes the steady-state current together with the Zero-Sequence Current Component (ZSCC) [39]. Winding taps allow the authors to create ITSCs with different fault severity levels. The results show an increase in the  $3f_s$  component in both current and ZSCC as the fault becomes more severe

and torque increases. In [40], the negative sequence of the current in  $dq$  frame is considered to identify low levels of fault severity. The proposed method utilizes the  $2f_s$  component as a fault indicator. In addition to the current signal, the ZSVC is used to detect ITSCs in [41]. The results show that ITSC faults generate an increase in the 5th harmonic in the stator current and an increase in the odd triple harmonics in the ZSVC spectrum. However, these methods are valid only for steady-state operating conditions. No literature on stator winding fault detection under non-stationary conditions in synchronous reluctance motors (SynRM) is found. Table 1 summarizes and classifies the stator winding short-circuit faults that are discussed in the present subsection.

**Table 1.** Classification of detection methods for stator short-circuit faults in PMSMs and SynRMs.

Type of Motor	Domain Classification	Reference	Signal Analyzed	Methodology	Regime	Advantages	Disadvantages
SynRM	Frequency-domain method	[38–40]	Current	FFT	Steady-state	NINV, EV	SIM [38], SSC
		[39]	ZSCC			NINV, EV	SSC
		[40]	Current in q-axis			NINV, EV	SSC
SynRM (PMAssisted)	Frequency-domain method	[41]	ZSVC	FFT	Steady-state	NINV, EV	SSC
	Time-domain method	[42]	Current	Waveform	*	NINV	SIM
PMSM	Frequency-domain method	[18–21,24,29,43]	Current	FFT	Steady-state	EV	SSC
		[23,43]		EPVA		EV	SSC
		[20,24]	Current envelope	FFT		EV	SSC
		[27,44]	ZSVC			EV	SSC
		[25]	Current negative sequence component	EV		SSC	
		[28]	Voltage in dq frame	BS		EV	SC
		[22]	Current			PSD	EV
		[29]	Speed	MUSIC		EV, HS	SSC
		[26]	Voltage	FFT		EV	SSC
		[17]		FFT		EV	SSC
		[19]		DWT		EV	SSC
		[30]	Current	STFT		EV, TA	Trade-off between t-f resolution
		[31,32]		HHT		EV, TA	
		[35,36]	ZSVC	DWT		EV, TA	
		[27]		HHT		EV, TA	Transient
[37]	Voltage in q-axis	DWT	EV, TA				
[33,34]	Current in q-axis	STFT	EV, TA	Trade-off between t-f resolution			
[45]	Current	Residual Analysis	EV, TA				
[46]	Back EMF		EV, TA				
[47]	Current	PCA	*	SIM			
[24]		RMS	Steady-state	EV	SSC		
[24]	Current envelope	Mean		EV	SSC		

EV: experimentally verified; SSC: steady-state condition; INV/NINV: invasive/non-invasive technique; VM: vibration measurement; TA: transient condition available; HCC/LCC: high/low computational cost; SIM: simulation only; AC: additional coil or sensor required; HS/LS: high/low sensitivity. \* Not specified.

## 2.2. Demagnetization Faults

Magnetic faults are related to the demagnetization of the rotor magnets in PMSMs and PMASynRMs. The demagnetization is induced by phenomena of different natures. An increase in temperature above the Curie temperature of the magnet causes the degradation of its inherent magnetic properties. In addition, exposure to an opposed magnetic field resulting from stator faults or uncontrolled transients can also result in demagnetization. Further causes leading to demagnetization are linked to corrosion and mechanical degradation [14]. The consequences of these faults are critical since the magnets directly contribute to the machine performance. Some of the side effects of demagnetization are increased torque ripple, Unbalanced Magnetic Pull (UMP), and unwanted noise and vibrations. The demagnetization can be partial or global, depending on the degradation angular location and/or the degree of demagnetization of each pole. The early detection of demagnetizing events is of capital importance to avoid further degradation of the machine magnets. A common methodology to detect demagnetization faults is the analysis of the phase current under steady-state operation [48–52] (i.e., MCSA). The literature identifies common fault indicator frequencies when the FFT is applied to the current signal [53]:

$$f_{dem} = f_s \left( 1 \pm \frac{k}{p} \right) \quad (2)$$

where  $f_s$  is the supply frequency,  $p$  is the number of pole pairs, and  $k = 1, 2, 3, \dots$

Demagnetization is not the only fault that can cause an increase in the frequencies given by (2). Eccentricity, misalignment, and imbalance faults share the same indicators. Thus, analysis of stator current is not appropriate since it cannot distinguish between different faults. The ZSCC is used in [50,54]. However, the technique presents the same drawbacks as MCSA. The same behavior is observed when using the ZSVC, as observed in [49,55]. The analysis of magnetic flux emerged as a powerful tool to accurately diagnose the demagnetization effect and prevent false diagnosis [56]. Harmonics in the current spectrum show that the 0.25th and 0.75th harmonics depend on operating speed, whereas the leakage flux components do not vary [57]. In [58], air-gap flux is used to diagnose demagnetization. In spite of its invasive nature, it is immune to the harmonics that are induced by power electronic devices. Further benefits of air-gap flux monitoring are non-dependency on the load condition and the possibility of diagnosing both partial and uniform demagnetization. Since flux density distribution is altered by demagnetization, back EMF is used for fault detection. The amplitude of high order EMF harmonics increases as observed in [59]. However, these are also affected by different phenomena and the demagnetization fault cannot be diagnosed. The variation of 5th and 7th harmonics is used in [60] as a fault indicator, where the harmonic content of the back-EMF spectrum is utilized for magnet fault detection but not experimentally verified. The utilization of FFT-based methodologies is limited to steady-state operation. The analysis of the transient regime of the machine represents an asset for fault discrimination and allows the diagnosis under non-stationary operation.

Current analysis is the most extended diagnosis methodology during transient regime. The detection of demagnetization during transient operation is mainly focused on PMSMs. Time–frequency signal processing tools such as wavelets or Hilbert–Huang transforms are commonly utilized. In [61], the DWT is used to evaluate the fault under different speeds and torque conditions. It is also used together with Continuous Wavelet Transform (CWT) in [62], where authors propose a method to reduce the dimensionality of data in the case of pure CWT. The advantages of the HHT are the easy implementation and the possibility of detection under different operating conditions [63,64]. The Wigner-Ville Distribution (WVD) provides better frequency resolution, but it is computationally expensive in comparison with other methods. In addition, the WCD presents a drawback related to the cross-terms that are inherent to this transform [65]. Signals of different nature are also analyzed by using time–frequency transformations, such as back EMF [66] or torque [67]. However, there is no information on whether the study is limited to the steady-state regime or can be

extended to the transient regime. Studies on demagnetization diagnosis in PMASynRMs cannot be found in the literature, even though increased research attention has recently been given to this machine topology. The methods used to detect demagnetization in PMSMs are summarized in Table 2.

**Table 2.** Classification of detection methods for demagnetization faults in PMSMs.

Type of Motor	Domain Classification	Reference	Signal Analyzed	Methodology	Regime	Advantages	Disadvantages	
PMSM	Frequency-domain method	[48–52]	Current	FFT	Steady-state	NINV, PD, EV	SSC, LS	
		[50,54]	ZSCC			PD, UD, HS, EV	INV, SSC	
		[49,55]	ZSVC			PD, HS, EV	INV, SSC	
		[57]	Leakage Flux			PD, UD, HS	INV, SSC	
		[58]	Air-gap Flux			PD, UD, HS	INV, SSC	
		[59,60,68]	Back EMF			NINV, UD [60], EV [59], PD [59]	SIM [60], SSC	
		[69]	Vibration			NINV, PD	SSC, VM	
	Time-frequency-domain method	[61,62,70]	Current	CWT/DWT	Transient	NINV, UD, EV		
		[65,67,71]		WVD		NINV, UD, EV		
		[72]		CWD		NINV, PD	HS	
		[63,64,73]		HHT		NINV, TA, PD, EV	HS	
		[66]		Back EMF		DWT	NINV, UD	
	Time-domain method	[67]	Torque	CWT and GST	*	NINV, PD, EV		
		[74]	Torque	TDE		NINV, PD, UD	LS	
		[75]	Back EMF	ZCP		NINV, PD, HS		
		[76]	ZSMC	Mean Peak		Steady-state	NINV, UD, EV	LS
		[77]	Current	VKF-OT		Transient	NINV, PD, HS, TA	

EV: experimentally verified; SSC: steady-state condition; INV/NINV: invasive/non-invasive technique; PD/UD: partial/uniform demagnetization; TA: transient condition available; HCC/LCC: high/low computational cost; SIM: simulation only; HS/LS: high/low sensitivity; VM: vibration measurement. \* Not specified.

### 2.3. Bearing Faults

Bearing damages represent around 41% of the machine faults in low voltage applications [14]. The most common bearing failure mechanisms are overloading, brinelling, assembly inaccuracies, lack of lubrication, partial discharge currents, contamination, etc. Vibration monitoring is the most common technique for bearing damage identification. However, frequency domain current analysis is a viable alternative for detecting faults in bearing elements, particularly in situations where vibration analysis is not feasible. Amplified components in the current spectrum are related to those obtained from vibration spectrum analysis. The different frequency components depend on the bearing geometry and on the location of the fault:

$$f_o = N_b \cdot \frac{f_r}{2} \cdot \left(1 - \frac{D_b \cos \theta}{D_p}\right) \quad (3)$$

$$f_i = N_b \cdot \frac{f_r}{2} \cdot \left(1 + \frac{D_b \cos \theta}{D_p}\right) \quad (4)$$

$$f_c = \frac{f_r}{2} \cdot \left(1 - \frac{D_b \cos \theta}{D_p}\right) \quad (5)$$

$$f_b = \frac{D_p}{D_b} \cdot f_r \cdot \left(1 - \left(\frac{D_b \cos \theta}{D_p}\right)^2\right) \quad (6)$$

where  $N_b$  is the number of balls,  $D_b$  is the rolling element diameter,  $D_p$  is the bearing pitch diameter,  $\theta$  is the bearing working angle,  $f_o$  is the frequency of outer race failures,  $f_i$  is the frequency of inner race failures,  $f_c$  is the frequency of bearing cage failures, and  $f_b$  is the frequency of ball defects.

The main fault indicators in the vibration frequency spectrum are given by the following equation:

$$f_{bea, v} = m \cdot f_{i,o} \pm k \cdot f_r \tag{7}$$

where  $f_{i,o}$  is the corresponding frequency in the vibration spectrum according to the location of the fault (Equations (3)–(6)),  $m = 1, 2, 3 \dots, k = 0, 1 \dots$ , and  $f_r$  is the rotational frequency. The frequency components in the current spectrum can be derived from the vibration characteristic frequencies by using the following expression:

$$f_{bea, c} = |f_s \pm m \cdot f_{i,o}| \tag{8}$$

where  $f_s$  is the supply frequency and  $m = 1, 2, 3 \dots$ . Fault harmonic indicators appear in the current spectrum with low amplitude, and threshold values are not yet specified to determine the fault severity.

Different works study bearing failures by using the FFT in vibration signals during steady-state operation [78–81]. In the case of transient analysis, the use of Order Analysis (OA) allows analysis during dynamic states [78,82]. The steady-state vibration spectrum envelope is utilized in different works, showing similar advantages and drawbacks as in the vibration spectrum case [78,81]. In addition, the transient analysis of the vibration envelope presents an added drawback, since it is capable of detecting only one type of bearing fault [83–85]. Several works utilize classic MSCA to detect different types of bearing damage. However, fault detection indicators are weaker than in the case of vibration signals, as shown in [79]. In [86,87], the proposed method shows poor sensitivity when the speed is reduced or torque variations occur. The DWT and CWT are applied to transient current signals in [87], where the results are experimentally verified. In the case of DTW, energy is utilized as fault indicator, while in the case of CWT, only the waveforms are analyzed in a qualitative diagnosis. In addition to current and vibration signals, stray flux is utilized to diagnose bearing faults. Gurusamy et al. [88] demonstrate that the stray flux frequency spectrum provides more interesting information about bearing faults than current or vibration spectra. No literature is found dealing with bearing fault diagnosis in SynRMs in either steady-state or transient operation. The presented works on bearing fault diagnosis in PMSMs are summarized in Table 3.

**Table 3.** Classification of detection methods for bearing faults in PMSMs.

Type of Motor	Domain Classification	Reference	Signal Analyzed	Methodology	Regime	Advantages	Disadvantages	
PMSM	Frequency-domain method	[79,86,87,89,90]	Current	FFT	Steady-state	NINV	SSC	
		[88]		OA	*	NINV, EV	OB, LS	
		[91]		ZFFT		NINV	SIM	
		[82]	Current EPVA	FFT	Steady-state		SSC, SIM	
				OA	Transient	NINV, TA		
		[78–82]	Vibration	FFT	Steady-state	NINV	SSC, VM	
		[78,82]		OA	Transient	NINV	OB, VM	
		[78,80,81,92]	Vibration Envelope	FFT	Steady-state	NINV	VM	
		[83–85,93,94]		OA		NINV, TA	VM	
		[95]	Noise	OA	Transient		TA, SIM and EV	VM
		[96]		FFT, OA				
		[88]	Stray Flux	OA	*	NINV, HS, EV	OB, AC	
		[97]	Speed Envelope	FFT	Steady-state	EV	SSC	

Table 3. Cont.

Type of Motor	Domain Classification	Reference	Signal Analyzed	Methodology	Regime	Advantages	Disadvantages
		[98]	Speed Vibration Current	FFT + Kurtosis Spectrum	*	Wide speed range	OB, VM
	Time–frequency- domain method	[87]	Current	DWT	Transient	NINV, EV, TA	VM
		[87]		CWT			
		[99]		STFT			
	Time domain method	[89,90]	Current	Statistical Features	*	NINV	

EV: experimentally verified; SSC: steady-state condition; INV/NINV: invasive/non-invasive technique; VM: vibration measurement; TA: transient condition available; HCC/LCC: high/low computational cost; SIM: simulation only; OB: one type of bearing fault; AC: additional coil or sensor required; HS/LS: high/low sensitivity. \* Not specified.

#### 2.4. Eccentricity Faults

Eccentricity in rotating machines is commonly defined as the offset between the center of rotation and the axis of symmetry. As a consequence, the air-gap width of the machine loses uniformity across its angular extension. Eccentricity may have an inherent nature resulting from inaccuracies during motor manufacturing and assembly, but it also arises as a consequence of operational faults such as shaft bow or bearing wear. The existence of eccentricity leads to asymmetrical stresses on different components of the machine, which contribute to a reduction in service life. No clear international consensus is found on the level of eccentricity at which maintenance action should be taken. However, it is assumed that the maximum allowed level of eccentricity should be around 10% [100]. Eccentricity is generally classified into three types. Static eccentricity (Figure 1a) takes place when the position of the minimum air gap remains fixed in space and is caused by mounting inaccuracies or an oval stator, among other causes. Dynamic eccentricity (Figure 1b) is found when the position of the minimum air gap is not fixed in space but changes with the angular position of the rotor. Possible causes of dynamic eccentricity are the presence of an oval rotor, bearing defects, etc. The mixed type of eccentricity (Figure 1c) is the most common, since a certain level of static and dynamic eccentricity is found in every machine due to inherent manufacturing tolerances.

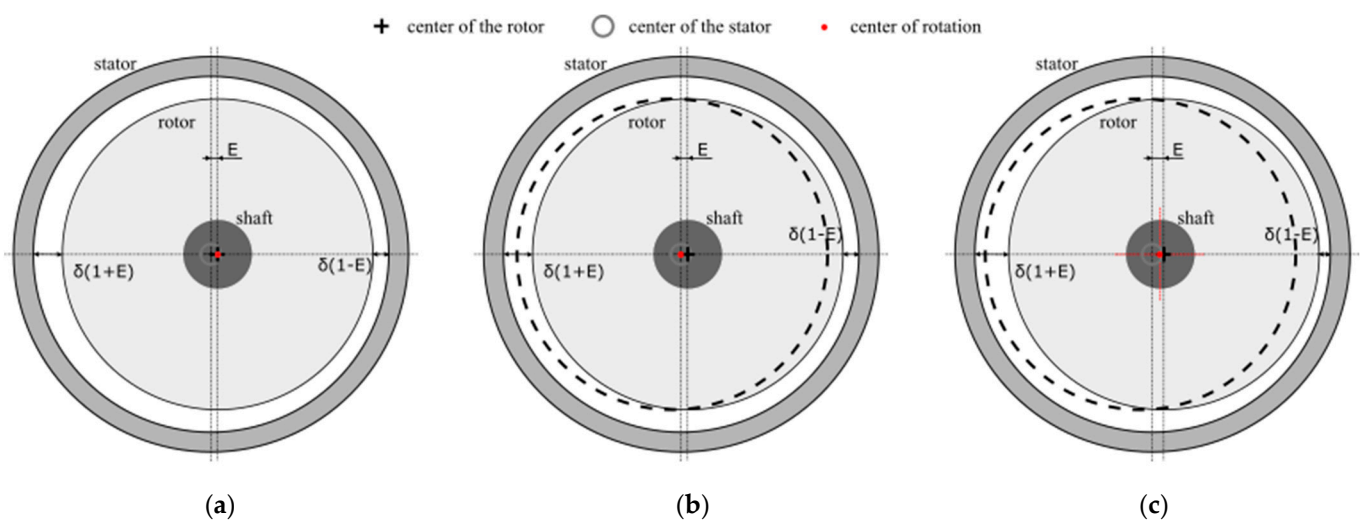


Figure 1. Eccentricity type description, (a) static, (b) dynamic, and (c) mixed.

The most common signal for eccentricity diagnosis is the phase current, in which additional frequency components appear when an eccentricity is present. These frequency components are given by [14]:

$$f_{ecc} = f_s \left( 1 \pm \frac{2k-1}{p} \right) \quad (9)$$

where  $k = 0, 1, 2, 3 \dots$

Eccentricity in PMSMs has attracted some research attention in recent years. The commonly utilized diagnostic signals are current [101–104], vibration [101,105], air-gap flux [101], torque [106], unbalance magnetic pull [107], and speed [106]. Analysis in the steady-state regime is performed using the FFT, where the study of the current spectrum shows an accentuation of frequencies around the rotation component. Air-gap flux is studied in [108] through FFT application, where an increase in 3rd- and 5th-order harmonics is observed.

The phase current is the only signal used thus far to detect eccentricity during transient operation. Time–frequency transforms such as CWT and DWT prove to be robust tools in the case of changes in speed and torque [109]. In addition, time-domain methods are widely used in eccentricity detection by using non-stationary signals. A widely used technique for monitoring changes in waveforms relies on observing changes in the different waveforms, with flux signals exhibiting significant potential [101,105]. Ahsanullah et al. [105] show how the study of the air-gap flux is more effective for the diagnosis of eccentricity than analysis of vibration during transient or asymmetric conditions. Moreover, different faults with similar indicators such as demagnetization or load unbalance are properly discriminated in [101].

Regarding pure synchronous reluctance motors, the literature on the detection of eccentricity faults is quite limited. The most widespread method to detect this fault is analysis of the stator current utilizing the FFT. In [110], the authors developed a mathematical model to detect static eccentricity, where a real machine was tested in the laboratory to validate the method. Static eccentricity revealed a higher amplitude in  $3f_s$  and  $-9f_s$  current harmonics. Furthermore, this work shows how to distinguish between the different types of eccentricity. In [111], the same authors extended their work with the objective of diagnosing any type of eccentricity fault. It is demonstrated that dynamic eccentricity accentuates the amplitude of  $5f_s$  and  $7f_s$  harmonics, whereas mixed eccentricity produces sideband harmonics around the fundamental and higher-order odd harmonics. In addition to current signals, back EMF harmonics are studied as a fault indicator. It is proven that the presence of eccentricity increases the amplitude of the 1st and 3rd order harmonics [112]. However, the study is limited to a FEM model, and has not been supported with experimental data. In Table 4, the diagnostic methods applied to PMSMs and SynRM are summarized.

**Table 4.** Classification of detection methods for eccentricity faults in PMSMs and SynRMs.

Type of Motor	Domain Classification	Reference	Signal Analyzed	Methodology	Regime	Advantages	Disadvantages
SynRM	Frequency-domain method	[110,111]	Current	FFT	Steady-state	NINV, EV, SE, DE and ME [111]	SSC
	Time-domain method	[113]	Torque Air-gap flux Radial Force	Waveform	*	NINV, SE and DE	SIM
SynRM (PMAssisted)	Frequency-domain method	[114]	Current ZSVC	FFT	Steady-state	NINV, SE	SSC, SIM
		[112]	Back EMF			NINV, SE, DE and ME	SSC, SIM
	Time-domain method	[112]	Torque ripple	Waveform	*	NINV	SIM

Table 4. Cont.

Type of Motor	Domain Classification	Reference	Signal Analyzed	Methodology	Regime	Advantages	Disadvantages
PMSM	Frequency-domain method	[101–104,115]	Current	FFT	Steady-state	NINV, EV	SSC, SIM [115]
		[116–118]		PSD		NINV, EV	SSC
		[106]		*	NINV, EV	SE	
		[101,105]	Vibration	FFT	Steady-state	NINV	SSC, VM
		[119]		FFT, OA	*	NINV, EV	VM, SIM (SE)
		[106]	Noise			NINV, EV	VM, SIM (SE)
	[106]	Voltage Speed Torque	PSD	*	EV	SE	
	[108]	Air-gap Flux	FFT	Steady-state	EV	NINV, DE	
	[120]	UMP		*	EV		
	Time–frequency-domain method	[109]		CWT	Transient	NINV, EV, TA	
		[86,109]	Current	DWT		NINV, TA, EV [109]	
		[118]			Steady-state	NINV, EV	SSC
	Time-domain method	[101,105]	Air-gap Flux	Waveform	*	INV, AC	
		[107]	UMP	Peak	Steady-state	EV	SSC, INV, AC
		[121,122]	Current in d-axis	Waveform	*	EV, HS	DE
		[118]	Current	PCA	Steady-state	NINV, EV	SSC, SE, DE
		[123]	Axial Flux	Waveform		EV	SSC, AC, INV

EV: experimentally verified; SSC: steady-state condition; INV/NINV: invasive/non-invasive technique; TA: transient condition available; HCC/LCC: high/low computational cost; SIM: simulation only; SE/DE/ME: static/dynamic/mixed eccentricity; HS/LS: high/low sensitivity; AC: additional coil or sensor required. \* Not specified.

### 2.5. Unbalance Faults

The phenomenon of unbalance occurs when the mass distribution of a rotating element is not uniform in relation to its axis of rotation. The result is the appearance of unbalanced centrifugal forces and moments that may damage several machine components. The unbalance depends on the rotational speed and thus, the increase in the amplitude of rotational frequencies serves as an indicator of this fault. A higher amplitude of  $f_r$  components is observed in the mechanical vibration spectrum, while the  $f_s \pm f_r$  frequencies are a fault indicator in the current spectrum.

In [124], the authors present high order methods to detect unbalance in drive systems with PMSMs. The vibration signal is analyzed through three different methodologies during the steady-state regime. FFT, BS and Full Spectrum (FS) processing methods are applied to obtain the value of the amplitude of characteristic harmonics. The BS analysis increases the detectability of unbalances. However, it requires an increased computational effort compared to FFT analysis. The FS requires the usage of at least two vibration sensors and a shaft position indicator. This method allows the detection during transient operation. Current measurement is widely used to diagnose unbalance faults in PMSMs drives. Hang et al. [125] analyze the current signal in the rotating reference frame to detect unbalances even during transient operation. Current-based methods for unbalance detection applied to PMSMs can be found in [126,127]. The different techniques to detect unbalance faults in PMSMs are summarized in Table 5.

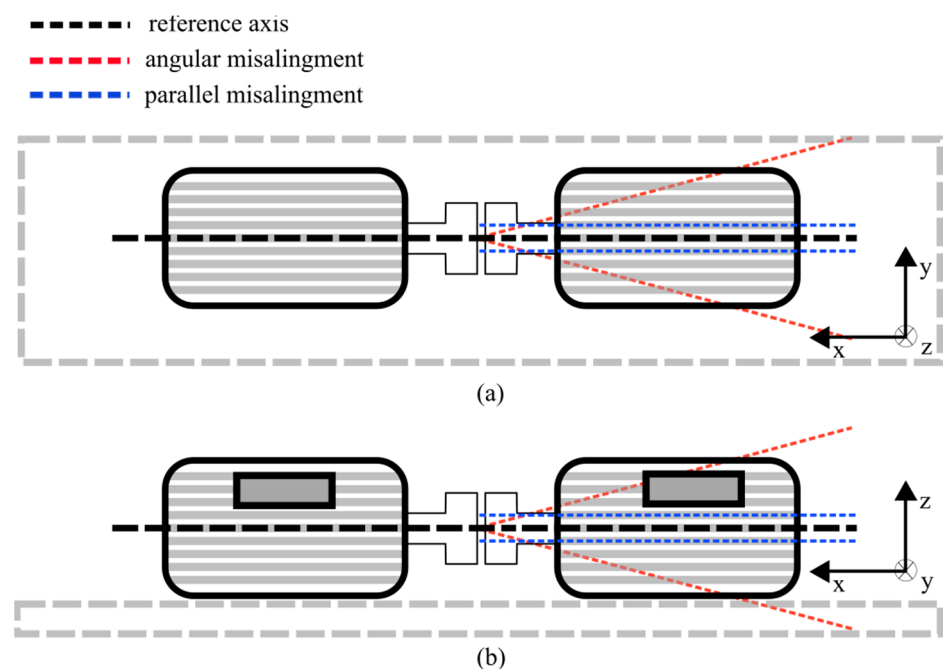
### 2.6. Misalignment Faults

Misalignment faults relate to the coupling between the motor and the load. They take place when the centerlines of the coupled shafts do not exactly coincide. Misalignment is divided into three types: parallel, angular, and a combination of both (Figure 2). The level of misalignment is hard to determine since there is no equipment to measure it.

**Table 5.** Classification of detection methods for rotor unbalance faults in drive systems with PMSMs.

Type of Motor	Domain Classification	Reference	Signal Analyzed	Methodology	Regime	Advantages	Disadvantages	
PMSM	Frequency-domain method	[124]	Vibration	FFT	Steady-state	NINV, EV, LCC	SSC, VM	
				BS		NINV, EV	SSC, VM	
				FS		NINV, EV, TA	SSC, VM, HCC	
	Time-frequency-domain method	[125]	Current EPVA	FFT	Transient	NINV, LCC	SSC, SIM	
				[126]		Vibration	NINV, EV	SSC, VM
				[125]		Current EPVA	DWT	NINV, TA
[127]	Current	CWT	NINV, TA	SIM				

EV: experimentally verified; SSC: steady-state condition; INV/NINV: invasive/non-invasive technique; VM: vibration measurement; TA: transient condition available; HCC/LCC: high/low computational cost; SIM: simulation only.

**Figure 2.** Misalignment fault description, (a) horizontal plane and (b) vertical plane.

The most widely used method to detect misalignment in PMSMs in the steady-state regime is current-based FFT analysis. It is demonstrated that changes in the rotational frequencies can be associated with misalignment faults. In [128,129], FFT analysis of the speed is used to detect misalignment. In addition, the amplitude of the  $2f_r$  component is used as a fault indicator. On the other hand, in [130], different methods of current analysis are compared: FFT, RMS, and DWT. Moreover, the stator current envelope and the space vector module are utilized for misalignment detection. The amplitude of the frequency component  $f_s + f_r$  increases its amplitude when misalignment exists, but it is strongly dependent on load torque. However, the  $f_r$  component in the stator current envelope or stator current module shows a weaker dependency on the motor operating conditions and it is a better indicator for diagnosis. DWT analysis shows that RMS values are sensitive to misalignment, but it is not suitable for misalignment detection due to its negligible sensitivity to the fault. However, the envelope and space vector modulus have less sensitivity to changes in operating conditions. FFT analysis is also employed with rotational speed in [128,129].

Regarding transient analysis, some studies have explored the use of stray flux signals as a means of detecting misalignment in induction motors, yielding promising outcomes. However, this method is applicable only to induction motors [131]. For synchronous

reluctance motors, there is no literature on misalignment detection in either the steady-state or transient regimen. The literature review regarding misalignment is summarized in Table 6.

**Table 6.** Classification of detection methods for rotor misalignment faults in PMSMs.

Type of Motor	Domain Classification	Reference	Signal Analyzed	Methodology	Regime	Advantages	Disadvantages
PMSM	Frequency-domain method	[130]	Current Current EPVA Current ENV	FFT	Steady-state	NINV	SSC, AM
		[128,129]	Speed			NINV, EV, AM and PM [129]	AM [128], SSC
	Time–frequency-domain method	[130]	Current Current EPVA Current ENV	DWT		NINV	SSC, AM
		[132]	Torque	Waveform		EV	PM, SSC
	Time-domain method	[133]	Current in q-axis	VPT		EV	SSC, AM
		[130]	Current	RMS		*	NINV

EV: experimentally verified; SSC: steady-state condition; AM/PM: angular/parallel misalignment; INV/NINV: invasive/non-invasive technique. \* Not specified.

### 3. Case Studies

The present section shows two different laboratory case studies to demonstrate the potential of transient regime analysis for a PMSM and a SynRM. In both cases the signal to be analyzed is the stator current, using a suitable time–frequency transform. STFT is a commonly utilized tool to obtain time–frequency maps at a limited computational cost. The present work discusses two different faults. Firstly, an eccentricity is studied during transient operation for a PMSM by manipulating the bearing configuration. Secondly, a misalignment fault is studied in a pure SynRM during the machine start-up.

#### 3.1. Short-Time Fourier Transform (STFT)

The Short-Time Fourier Transform (STFT) is a linear transform that correlates a signal with a set of time–frequency atoms. A time–frequency atom consists of a function whose energy is concentrated at a point in the time–frequency map. Therefore, the energy distribution of the signal is obtained by correlating the studied signal with the different time–frequency atoms within the time–frequency map.

The STFT divides the signal into small segments, which can be assumed to be stationary. The segmentation of the signal is performed by utilizing a time window function. The length of the window coincides with the selected length for the different signal segments. Thus, the window function  $w(t - \tau)$  and the signal  $x(t)$  are multiplied considering half period of the chosen signal. Finally, the FFT is performed on the result of the product. The STFT is described by the following expression:

$$STFT\{x(t)\} \equiv X(\tau, f) = \int_{-\infty}^{\infty} x(t) \cdot w(t - \tau) \cdot e^{-j2\pi ft} dt \quad (10)$$

where  $\tau$  defines the location of the time window.

The main drawback of the STFT is that the exact time–frequency representation of a signal cannot be precisely known. The time interval is always discrete, covering only a part of the signal. The discrete nature of the transform sets a trade-off between time and frequency resolution, where increased resolution in the time frequency domain is obtained for larger time windows and vice versa. Therefore, it is necessary to find the most suitable window size for the considered application.

#### 3.2. Eccentricity in PMSM

The first laboratory test deals with an eccentricity fault induced in a surface-mounted PMSM utilized in fluid pumping applications. Table 7 includes the characteristics of the

studied machine. It is directly connected to a fluid load emulator, where the impeller of the pump is connected to a system consisting of five parallel vertical pipes with a diameter of DN100. To control the load, suitable pressure sensors are installed in the piping system. The motor is fed by using an embedded variable-frequency drive (VFD), which is user controlled by a custom interface. The phase current is precisely monitored by dedicated current sensors connected to an acquisition board with a sampling frequency of 10 kHz. In addition, a power analyzer is utilized to obtain machine operating parameters such as voltage, absorbed current, power factor, etc. Figure 3 shows the laboratory test bench highlighting the main elements of the setup.

**Table 7.** Main characteristics of the pump.

Power	0.8 kW
Nominal head	18 m
Speed range	1000–3400 rpm
Number of impeller blades	7
Pole pairs	4

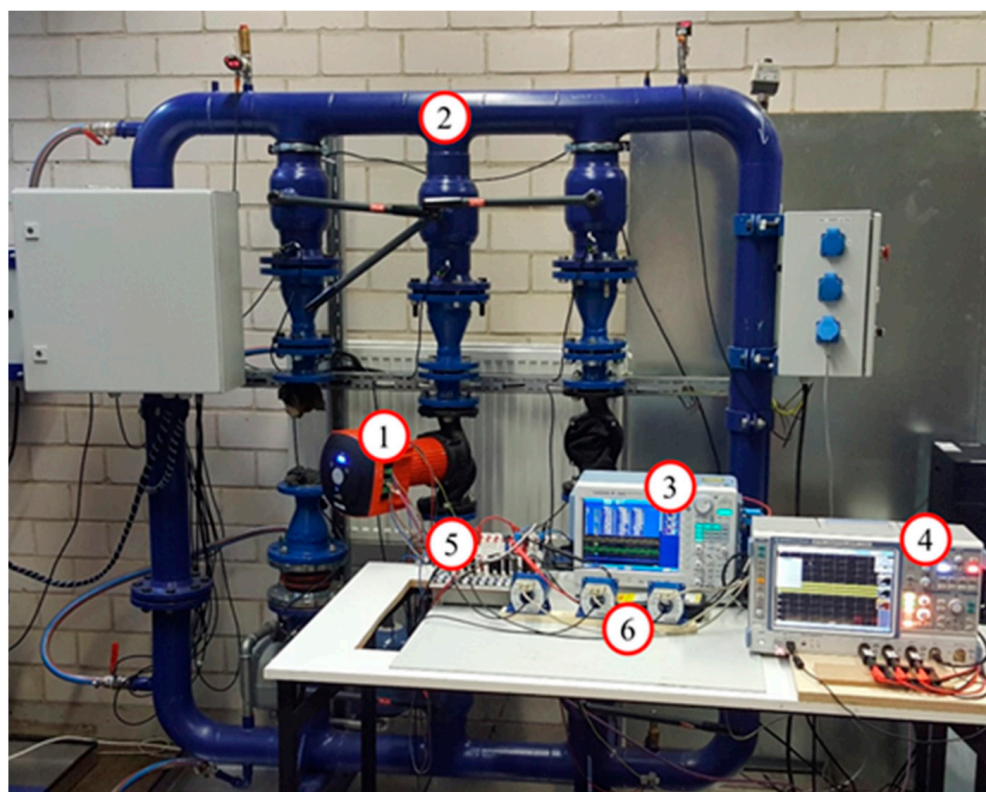


**Figure 3.** PMSM test bench for eccentricity fault emulation. (1) PMSM, machine under study, (2) piping system, (3) power analyzer, (4) waveform recorder, (5) acquisition board and (6) current sensors.

The eccentricity fault is induced by modifying the bearing bushes. In this case, the motor is part of a wet-rotor pump, where the utilization of journal bearings is highly recommended. The bearings of the pump are accessed by removing the impeller and the VFD from the main housing and by separating the impeller from the shaft. The bushing of the two bearings is ground down by 0.2 mm by utilizing a lathe to induce the fault. Figure 4 shows the location of the bearings and the change in inner radius after manipulation.

The test is performed by changing the machine speed, which directly impacts the location of the fundamental frequency. Figure 5 shows the time–frequency maps obtained via STFT for the studied machine under healthy and faulty conditions during the period

where the speed is varied. An immediate observation is that the components located in  $f_s \pm f_r$  arise as a result of the fault. The component located at  $f_s - f_r$  is visible during the transient and steady-state regimes for both operational speeds. However, the component located at  $f_s + f_r$  is visible only during the second operational speed. Therefore, the frequencies around the fundamental frequency located at  $f_s \pm f_r$  can be utilized as a fault indicator for eccentricity in PMSMs during transient operation. The present laboratory work further validates the results presented in [86,109]. In addition, it demonstrates the validity of bearing-bushing modification to induce eccentricity.

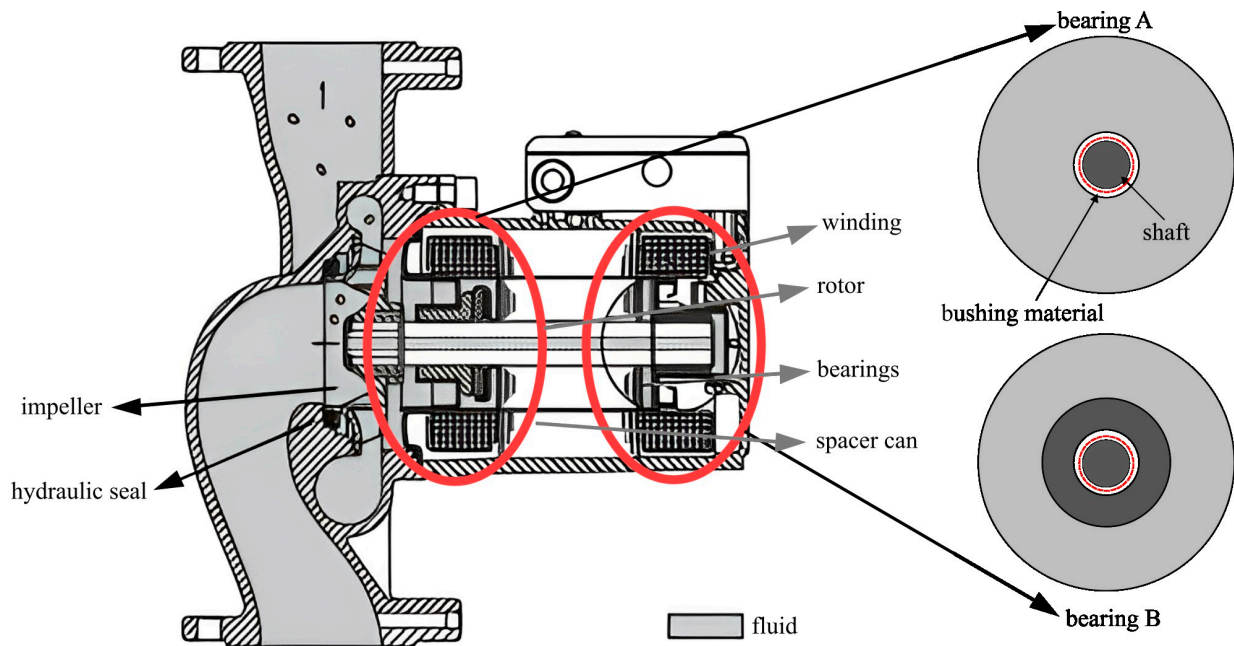


Figure 4. Pump diagram [134] and description of the utilized journal bearing including degradation description.

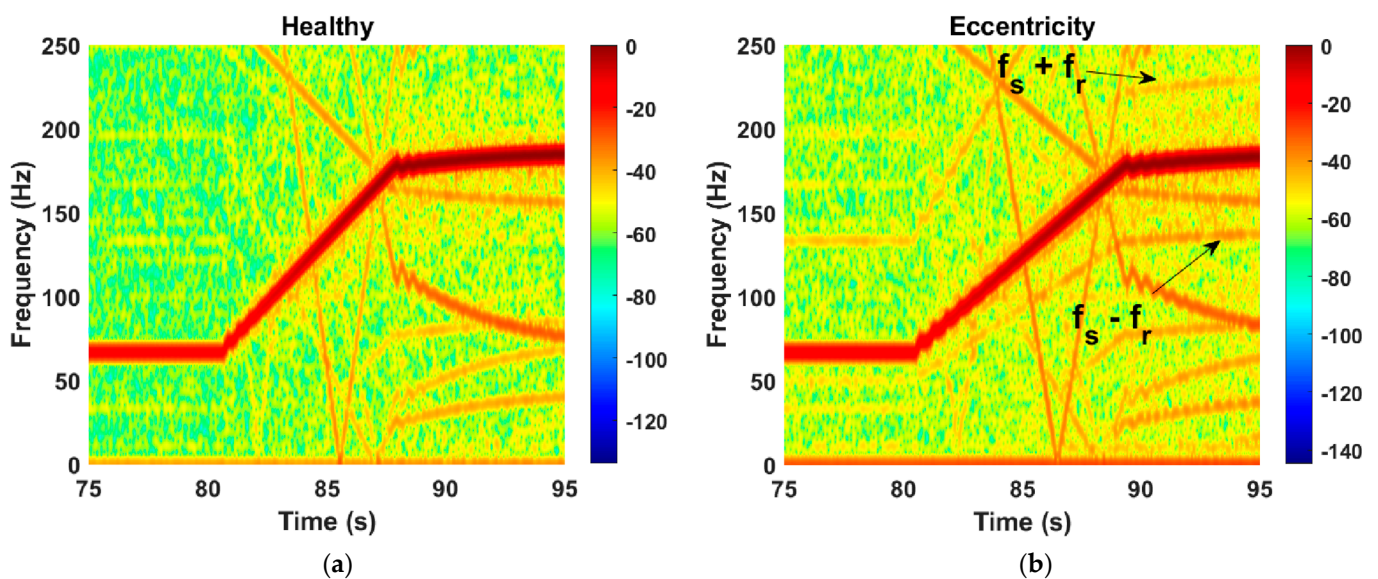


Figure 5. STFT analysis of PMSM, (a) Healthy motor and (b) motor with eccentricity.

### 3.3. Misalignment in SynRM

Misalignment fault diagnosis tests are carried out in a two-pole pair, 1.1 kW pure SynRM. Table 8 shows the case-study machine characteristics. The motor is coupled to a DC

generator acting as a load, where the field excitation is regulated to impose different levels of resistant torque. The motor is fed via a VFD programmed to maintain a fixed speed. Figure 6 shows the test bench in the laboratory. In the case of the healthy condition, the motor is aligned with the load by using a proper alignment tool that measures the relative position of the motor axis with respect to the load axis both vertically and horizontally. The tool shows the rotation axis position and estimates the offset between the motor and the load axes. To emulate the fault, the misalignment is forced by using two shims on the back motor mountings. Figure 7a shows the faulty mountings and Figure 7b shows the disassembled shims. Current signals are captured using suitable current clamps connected to a waveform recorder both during the motor startup (10 s) and in steady-state conditions using a sampling rate of 10 kHz. The characteristics of the SyRM are shown in Table 8.

**Table 8.** Main characteristics of the SynRM.

Power	1.1 kW
Voltage	360 V—star connection
Nominal Current	3 A
Nominal torque	7 Nm
Base speed	1500 rpm
Pole pairs	2

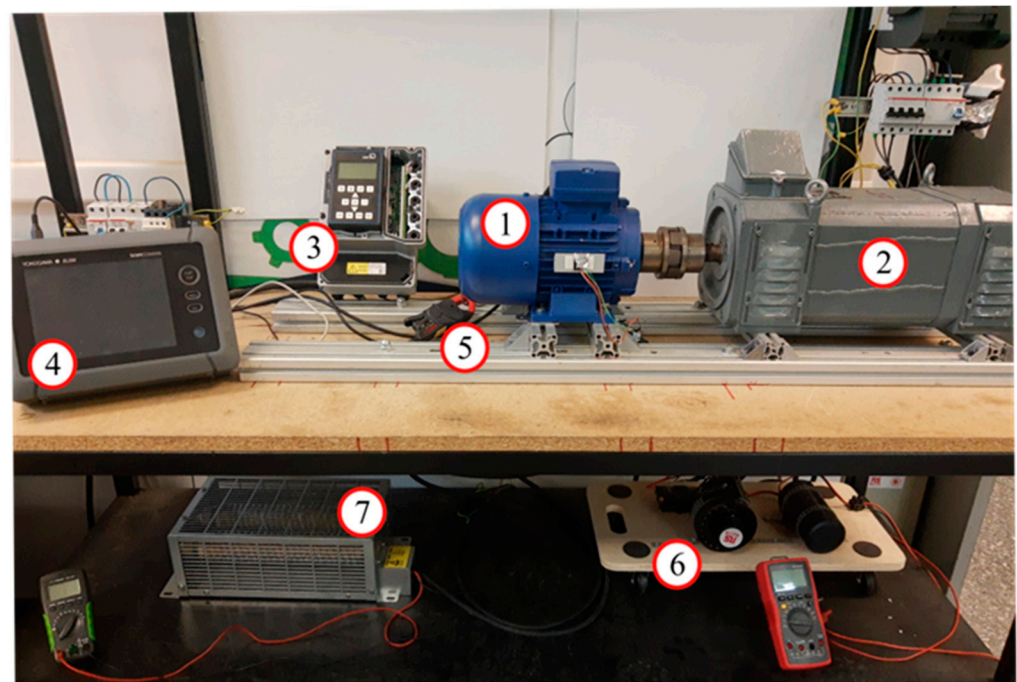


**Figure 6.** SynRM test bench for misalignment fault emulation. (1) SynRM, machine under study, (2) DC generator, (3) VFD, (4) Waveform recorder, (5) Current clamp, (6) Field excitation regulator, (7) Dissipative load.

Figure 8a shows the STFT results for the healthy condition of the motor both in the transient regime and at steady state, where the color map represents the energy density normalized to the fundamental component. Rotational frequencies given by  $f_s \pm f_r$  appear with very low amplitude. The components start in 0 Hz and evolve following their expected trajectory across the startup duration. The existence of these frequencies in the healthy state of the motor is explained by inherent eccentricity due to manufacturing and assembly processes. Figure 8b shows the STFT results for the misaligned setup. An increase in the amplitude of the  $f_s \pm f_r$  components with respect to the healthy state of the motor is observed, which is visible not only at steady state but also during the startup transient regime. The

comparison between the two graphs highlights the amplitude accentuation of the  $f_s \pm f_r$  components when misalignment is present. Moreover, analysis of the transient regime provides additional information about the fault indicators evolution, thus contributing to the reliability of misalignment fault detection and discrimination.

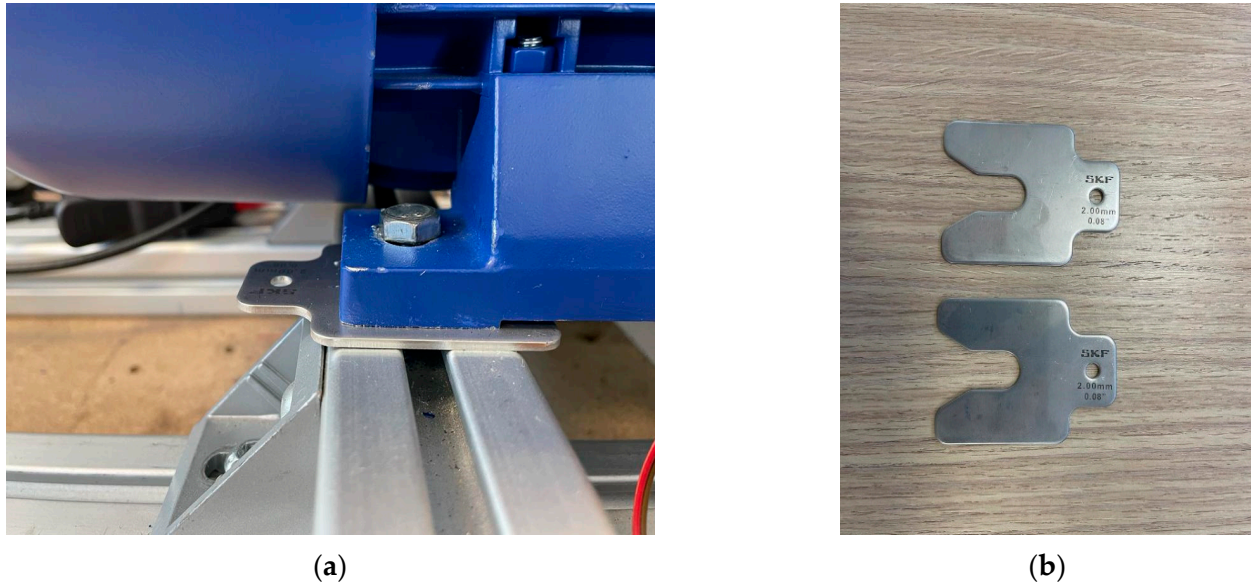


Figure 7. (a) Shim on the back SynRM mounting, (b) 2 mm shims used to force misalignment in the SynRM.

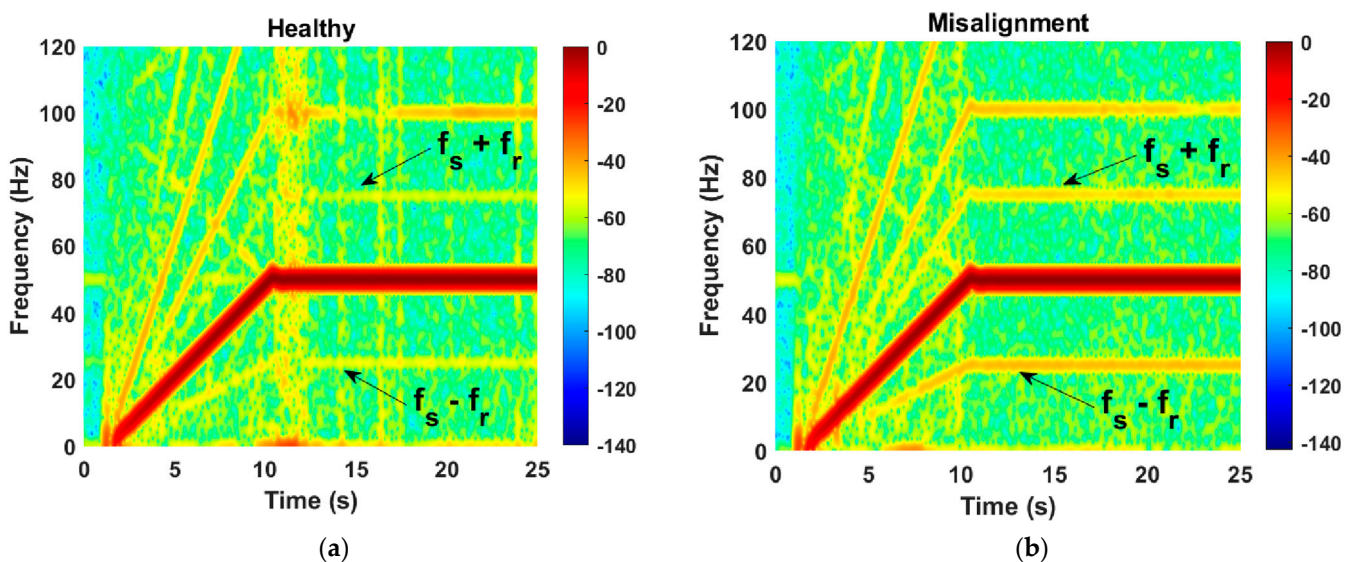


Figure 8. STFT analysis of SynRM, (a) Healthy motor and (b) motor with certain level of misalignment.

These case studies are intended to show, in a preliminary way, the potential of transient analysis to detect different faults, not only in PMSMs but also in SynRMs. The ability to identify fault components in time–frequency maps when a fault is present, and to observe an increase in their amplitude as the fault deteriorates, represents a promising approach for fault detection in SynRMs. The evaluation of energy distribution in strategic regions of the time–frequency maps is a promising tool for misalignment fault severity indication, as demonstrated previously for induction machines.

#### 4. Conclusions

The present work discusses the potential of fault detection techniques under non-stationary conditions in low- and medium-power synchronous machines. The literature review highlights deficiencies in the field, especially in the application to synchronous reluctance machines. Stator winding short circuits and eccentricity faults are the most studied type of failures in SynRM and PMASynRM. In these cases, fault detection is based on signal current analysis through frequency domain transforms, in particular the FFT which is limited to steady-state conditions. Regarding PMSMs, the literature review shows that stator winding short circuits and eccentricity faults are the most studied. However, only few works deal with the detection of these faults in transient conditions.

Furthermore, two laboratory case studies are presented to further demonstrate the potential of transient analysis applied to the machines at hand. First, eccentricity in a surface-mounted PMSM is studied over a speed transition. The second example analyzes the startup current to detect certain level of misalignment in a SynRM. Both case studies prove the potential of transient regime analysis to detect different types of faults in PMSMs and SynRMs. The results show qualitative changes in the rotational frequency components when the fault is present.

Based on the analysis carried out in this work, several research lines can be immediately identified for the future:

- A significant number of faults can be studied in SynRMs since, as discussed above, studies on these machines regarding condition monitoring have been quite scarce. In particular, transient analysis suitability can be investigated, since it has shown an excellent performance for other machines (such as induction motors or even PMSMs). The results included in this work also prove the potential of transient analysis for determining the condition of SynRMs.
- There is a need to deepen the development of fault severity indicators that are suitable both for PMSMs and SynRMs; unlike what happens in induction motors, where reliable fault indicators have been well established for some faults, and are used in the field, there are no reliable indicators for determining fault severity in PMSMs or SynRMs, which is a drawback when trying to apply new methodologies in the field.
- Extension of the newly developed methods to PMASynRMs is an immediate step forward, after the development of new methods in PMSMs and SynRMs, since these machines combine the main features of both machine typologies.
- Combination of the application of transient analysis methods not only to currents but also to other quantities such as stray fluxes is essential. This combination has proven to be helpful in discriminating between different faults (e.g., eccentricities and misalignments) in other types of machines (e.g., induction machines) and it would be of great value to analyze its suitability for fault discrimination in PMSMs and SynRMs.

**Author Contributions:** Conceptualization, A.N.-N., J.E.R.-S. and J.A.A.-D.; methodology, A.N.-N., J.E.R.-S., V.B.-M. and J.A.A.-D.; software, A.N.-N., V.B.-M. and V.B.; validation, A.N.-N., V.B.-M., V.B. and J.E.R.-S.; formal analysis, A.N.-N., J.E.R.-S., J.A.A.-D.; investigation, A.N.-N., J.E.R.-S.; resources, J.A.A.-D.; data curation, A.N.-N., V.B.-M., J.E.R.-S., V.B.; writing—original draft preparation, A.N.-N., J.E.R.-S.; writing—review and editing, J.E.R.-S., J.A.A.-D., V.B. and S.U.; visualization, A.N.-N., J.E.R.-S. and J.A.A.-D.; supervision, J.A.A.-D. and S.U.; project administration, J.A.A.-D. and S.U.; funding acquisition, J.A.A.-D. and S.U. All authors have read and agreed to the published version of the manuscript.

**Funding:** This research was funded by the Spanish ‘Ministerio de Ciencia e Innovación’, Agencia Estatal de Investigación and FEDER program in the framework of the ‘Proyectos de Generación de Conocimiento 2021’ of the ‘Programa Estatal para Impulsar la Investigación Científico-Técnica y su Transferencia’, belonging to the ‘Plan Estatal de Investigación Científica, Técnica y de Innovación 2021–2023’. (ref: PID2021-122343OB-I00).

**Conflicts of Interest:** The authors declare no conflict of interest.

## Abbreviations

BS	Bispectrum
CWT	Continuous Wavelet transform
DWT	Discrete Wavelet transform
EPVA	Extended Park vector analysis
GST	Grey system theory
HHT	Hilbert–Huang transform
ITSC	Inter-turn short-circuit
FFT	Fast Fourier transform
FS	Full spectrum
MCSA	Motor current signature analysis
MUSIC	Multiple signal classification
OA	Order analysis
PCA	Principal component analysis
PMASynRM	Permanent magnet assisted synchronous reluctance machine
PMSM	Permanent magnet synchronous machine
PSD	Power spectrum density
RMS	Root mean square
STFT	Short-time Fourier transform
SynRM	Synchronous reluctance machine
TDE	Time delay embedding
UMB	Unbalance magnetic pull
VFD	Variable-frequency drive
VKT-OT	Vold-Kalman filtering order tracking
VPT	Virtual phase torque
WVD	Wigner-Ville distribution
ZCP	Zero crossing point
ZFFT	Zoom FFT
ZSCC	Zero-sequence current component
ZSMC	Zero-sequence magnetic flux density component
ZSVC	Zero-sequence voltage component

## References

1. Mecrow, B.C.; Jack, A.G. Efficiency trends in electric machines and drives. *Energy Policy* **2008**, *36*, 4336–4341. [[CrossRef](#)]
2. Tsao, J.Y.; Schubert, E.F.; Fouquet, R.; Lave, M. The electrification of energy: Long-term trends and opportunities. *MRS Energy Sustain.* **2018**, *5*, 1–15. [[CrossRef](#)]
3. Pellegrino, G.; Vagati, A.; Boazzo, B.; Guglielmi, P. Comparison of induction and PM synchronous motor drives for EV application including design examples. *IEEE Trans. Ind. Appl.* **2012**, *48*, 2322–2332. [[CrossRef](#)]
4. De Gennaro, M.; Jürgens, J.; Zanon, A.; Gragger, J.; Schlemmer, E.; Fricassè, A.; Marengo, L.; Ponick, B.; Olabarri, E.T.; Kinder, J.; et al. Designing, prototyping and testing of a ferrite permanent magnet assisted synchronous reluctance machine for hybrid and electric vehicles applications. *Sustain. Energy Technol. Assess.* **2019**, *31*, 86–101. [[CrossRef](#)]
5. Donaghy-Spargo, C. Synchronous reluctance motor technology: Industrial opportunities, challenges and future direction. *Eng. Technol. Ref.* **2016**, *44*, 1–15. [[CrossRef](#)]
6. Lee, S.B.; Stone, G.C.; Antonino-Daviu, J.; Gyftakis, K.N.; Strangas, E.G.; Maussion, P.; Platero, C.A. Condition Monitoring of Industrial Electric Machines: State of the Art and Future Challenges. *IEEE Ind. Electron. Mag.* **2020**, *14*, 158–167. [[CrossRef](#)]
7. Shin, S.; Kim, J.; Lee, S.B.; Lim, C.; Wiedenbrug, E.J. Evaluation of the Influence of Rotor Magnetic Anisotropy on Condition Monitoring of Two-Pole Induction Motors. *IEEE Trans. Ind. Appl.* **2015**, *51*, 2896–2904. [[CrossRef](#)]
8. Antonino, J.A.; Riera, M.; Roger-Folch, J.; Molina, M.P. Validation of a new method for the diagnosis of rotor bar failures via wavelet transformation in industrial induction machines. In Proceedings of the 2005 5th IEEE International Symposium on Diagnostics for Electric Machines, Power Electronics and Drives, Vienna, Austria, 7–9 September 2005; Volume 42, pp. 990–996. [[CrossRef](#)]
9. Zamudio-Ramirez, I.; Osornio-Rios, R.A.; Antonino-Daviu, J.A. Smart Sensor for Fault Detection in Induction Motors Based on the Combined Analysis of Stray-Flux and Current Signals: A Flexible, Robust Approach. *IEEE Ind. Appl. Mag.* **2022**, *28*, 56–66. [[CrossRef](#)]
10. Yang, C.; Lee, S.B.; Jang, G.; Kim, S.; Jung, G.; Lee, J.; Shim, S.; Lim, Y.K.; Kim, J.; Park, S. Starting current analysis in medium voltage induction motors: Detecting rotor faults and reactor starting defects. *IEEE Ind. Appl. Mag.* **2019**, *25*, 69–79. [[CrossRef](#)]

11. Antonino-Daviu, J. Electrical monitoring under transient conditions: A new paradigm in electric motors predictive maintenance. *Appl. Sci.* **2020**, *10*, 6137. [[CrossRef](#)]
12. Climente-Alarcon, V.; Antonino-Daviu, J.A.; Vedreño-Santos, F.; Puche-Panadero, R. Vibration transient detection of broken rotor bars by PSH sidebands. *IEEE Trans. Ind. Appl.* **2013**, *49*, 2576–2582. [[CrossRef](#)]
13. Ramirez-Nunez, J.A.; Antonino-Daviu, J.A.; Climente-Alarcon, V.; Quijano-Lopez, A.; Razik, H.; Osornio-Rios, R.A.; Romero-Troncoso, R.D.J. Evaluation of the Detectability of Electromechanical Faults in Induction Motors Via Transient Analysis of the Stray Flux. *IEEE Trans. Ind. Appl.* **2018**, *54*, 4324–4332. [[CrossRef](#)]
14. Orłowska-Kowalska, T.; Wolkiewicz, M.; Pietrzak, P.; Skowron, M.; Ewert, P.; Tarchala, G.; Krzysztofiak, M.; Kowalski, C.T. Fault Diagnosis and Fault-Tolerant Control of PMSM Drives-State of the Art and Future Challenges. *IEEE Access* **2022**, *10*, 59979–60024. [[CrossRef](#)]
15. Urresty, J.; Riba, J.; Romeral, L.; Saavedra, H. Analysis of demagnetization faults in surface-mounted permanent magnet synchronous with inter-turns and phase-to-ground short-circuits. In Proceedings of the 2012 20th International Conference on Electrical Machines, Marseille, France, 2–5 September 2012; pp. 2384–2389. [[CrossRef](#)]
16. Gu, B.G.; Choi, J.H.; Jung, I.S. Development and analysis of interturn short fault model of PMSMs with series and parallel winding connections. *IEEE Trans. Power Electron.* **2014**, *29*, 2016–2026. [[CrossRef](#)]
17. Haddad, R.Z.; Strangas, E.G. Fault detection and classification in permanent magnet synchronous machines using Fast Fourier Transform and Linear Discriminant Analysis. In Proceedings of the 2013 9th IEEE International Symposium on Diagnostics for Electric Machines, Power Electronics and Drives (SDEMPED), Valencia, Spain, 7–30 August 2013; pp. 99–104. [[CrossRef](#)]
18. Ebrahimi, B.M.; Faiz, J. Feature extraction for short-circuit fault detection in permanent-magnet synchronous motors using stator-current monitoring. *IEEE Trans. Power Electron.* **2010**, *25*, 2673–2682. [[CrossRef](#)]
19. Rosero, J.; Garcia, A.; Cusido, J.; Romeral, L.; Ortega, J.A. On the short-circuiting Fault Detection in a PMSM by means of Stator Current Transformations. In Proceedings of the 2007 IEEE Power Electronics Specialists Conference, Orlando, FL, USA, 17–21 June 2007; pp. 1936–1941. [[CrossRef](#)]
20. Pietrzak, P.; Wolkiewicz, M. Comparison of selected methods for the stator winding condition monitoring of a pmsm using the stator phase currents. *Energies* **2021**, *14*, 1630. [[CrossRef](#)]
21. Romeral, L.; Urresty, J.C.; Riba Ruiz, J.R.; Garcia Espinosa, A. Modeling of surface-mounted permanent magnet synchronous motors with stator winding interturn faults. *IEEE Trans. Ind. Electron.* **2011**, *58*, 1576–1585. [[CrossRef](#)]
22. Rosero, J.; Ortega, J.; Urresty, J.; Cárdenas, J.; Romeral, L. Stator Short Circuits Detection in PMSM by means of Higher Order Spectral Analysis (HOSA). In Proceedings of the 2009 Twenty-Fourth Annual IEEE Applied Power Electronics Conference and Exposition, Washington, DC, USA, 15–19 February 2009; pp. 964–969. [[CrossRef](#)]
23. Fonseca, D.S.B.; Santos, C.M.C.; Cardoso, A.J.M. Stator Faults Modeling and Diagnostics of Line-Start Permanent Magnet Synchronous Motors. *IEEE Trans. Ind. Appl.* **2020**, *56*, 2590–2599. [[CrossRef](#)]
24. Pietrzak, P.; Wolkiewicz, M. Application of Support Vector Machine to stator winding fault detection and classification of permanent magnet synchronous motor. In Proceedings of the 2021 IEEE 19th International Power Electronics and Motion Control Conference (PEMC), Gliwice, Poland, 25–29 April 2021; pp. 880–887. [[CrossRef](#)]
25. Çıra, F.; Arkan, M.; Gümüş, B.; Goktas, T. Analysis of stator inter-turn short-circuit fault signatures for inverter-fed permanent magnet synchronous motors. In Proceedings of the IECON 2016—42nd Annual Conference of the IEEE Industrial Electronics Society, Florence, Italy, 23–26 October 2016; pp. 1453–1457. [[CrossRef](#)]
26. Cai, B.; Zhao, Y.; Liu, H.; Xie, M. A Data-Driven Fault Diagnosis Methodology in Three-Phase Inverters for PMSM Drive Systems. *IEEE Trans. Power Electron.* **2017**, *32*, 5590–5600. [[CrossRef](#)]
27. Urresty, J.C.; Riba, J.R.; Saavedra, H.; Romeral, L. Detection of inter-turns short circuits in permanent magnet synchronous motors operating under transient conditions by means of the zero sequence voltage. In Proceedings of the 2011 14th European Conference on Power Electronics and Applications, Birmingham, UK, 30 August–1 September 2011.
28. Ahn, G.; Lee, J.; Park, C.H.; Youn, M.; Youn, B.D. Inter-turn Short Circuit Fault Detection in Permanent Magnet Synchronous Motors Based on Reference Voltage. In Proceedings of the 2019 IEEE 12th International Symposium on Diagnostics for Electrical Machines, Power Electronics and Drives (SDEMPED), Toulouse, France, 27–30 August 2019; pp. 245–250. [[CrossRef](#)]
29. Krzysztofiak, M.; Skowron, M.; Orłowska-Kowalska, T. Analysis of the impact of stator inter-turn short circuits on pmsm drive with scalar and vector control. *Energies* **2021**, *14*, 153. [[CrossRef](#)]
30. Rosero, J.; Cusido, J.; Garcia, A.; Romeral, L.; Ortega, J.A. Detection of stator short circuits in PMSM by mean of joint time-frequency analysis. In Proceedings of the 2007 IEEE International Symposium on Diagnostics for Electric Machines, Power Electronics and Drives, Cracow, Poland, 6–8 September 2007; pp. 420–425. [[CrossRef](#)]
31. Urresty, J.; Riba, J.; Romeral, L.; Rosero, J.; Serna, J. Stator Short Circuits Detection in PMSM by means of Hilbert-Huang transform and energy calculation. In Proceedings of the 2009 IEEE International Symposium on Diagnostics for Electric Machines, Power Electronics and Drives, Cargese, France, 31 August–3 September 2009. [[CrossRef](#)]
32. Alvarez-Gonzalez, F.; Griffo, A.; Wang, B. Permanent magnet synchronous machine stator windings fault detection by Hilbert-Huang transform. *J. Eng.* **2019**, *2019*, 3505–3509. [[CrossRef](#)]
33. Strangas, E.G.; Aviyente, S.; Zaidi, S.S.H. Time-frequency analysis for efficient fault diagnosis and failure prognosis for interior permanent-magnet AC motors. *IEEE Trans. Ind. Electron.* **2008**, *55*, 4191–4199. [[CrossRef](#)]

34. Zanardelli, W.G.; Strangas, E.G.; Aviyente, S. Identification of intermittent electrical and mechanical faults in permanent-magnet AC drives based on time-frequency analysis. *IEEE Trans. Ind. Appl.* **2007**, *43*, 971–980. [[CrossRef](#)]
35. Fang, J.; Sun, Y.; Wang, Y.; Wei, B.; Hang, J. Improved ZSVC-based fault detection technique for incipient stage inter-turn fault in PMSM. *IET Electr. Power Appl.* **2019**, *13*, 2015–2026. [[CrossRef](#)]
36. Hang, J.; Zhang, J.; Xia, M.; Ding, S.; Hua, W. Interturn Fault Diagnosis for Model-Predictive-Controlled-PMSM Based on Cost Function and Wavelet Transform. *IEEE Trans. Power Electron.* **2020**, *35*, 6405–6418. [[CrossRef](#)]
37. Obeid, N.H.; Boileau, T.; Nahid-Mobarakeh, B. Modeling and diagnostic of incipient interturn faults for a three-phase permanent magnet synchronous motor. *IEEE Trans. Ind. Appl.* **2016**, *52*, 4426–4434. [[CrossRef](#)]
38. Neti, P.; Nandi, S. Stator Inter-turn Fault Analysis of Reluctance Synchronous Motor. In Proceedings of the Canadian Conference on Electrical and Computer Engineering, Saskatoon, SK, Canada, 1–4 May 2005; pp. 1283–1286. [[CrossRef](#)]
39. Henriques, K.; Laadjal, K.; Cardoso, A.J.M. Inter-Turn Short-Circuit Fault Detection in Synchronous Reluctance Machines, Based on Current Analysis. *Eng. Proc.* **2022**, *24*, 23. [[CrossRef](#)]
40. Mahmoudi, A.; Jlassi, I.; Cardoso, A.J.M.; Yahia, K.; Sahraoui, M. Inter-Turn Short-Circuit Faults Diagnosis in Synchronous Reluctance Machines, Using the Luenberger State Observer and Current's Second-Order Harmonic. *IEEE Trans. Ind. Electron.* **2021**, *69*, 8420–8429. [[CrossRef](#)]
41. Candelo-Zuluaga, C.; Riba, J.R.; López-Torres, C.; Garcia, A. Detection of inter-turn faults in multi-phase ferrite-PM assisted synchronous reluctance machines. *Energies* **2019**, *12*, 2733. [[CrossRef](#)]
42. Lare, P.; Sarabi, S.; Delpha, C.; Nasr, A.; Diallo, D. Stator winding Inter-turn short-circuit and air gap eccentricity fault detection of a Permanent Magnet-Assisted Synchronous Reluctance Motor in Electrified vehicle. In Proceedings of the 2021 24th International Conference on Electrical Machines and Systems (ICEMS), Gyeongju, Republic of Korea, 31 October–3 November 2021; pp. 932–937. [[CrossRef](#)]
43. Shamsi Nejad, M.A.; Taghipour, M. Inter-turn stator winding fault diagnosis and determination of fault percent in PMSM. In Proceedings of the 2011 IEEE Applied Power Electronics Colloquium (IAPEC), Johor Bahru, Malaysia, 18–19 April 2011; pp. 128–131. [[CrossRef](#)]
44. Urresty, J.C.; Riba, J.R.; Romeral, L. Diagnosis of interturn faults in pmsms operating under nonstationary conditions by applying order tracking filtering. *IEEE Trans. Power Electron.* **2013**, *28*, 507–515. [[CrossRef](#)]
45. Leboeuf, N.; Boileau, T.; Nahid-Mobarakeh, B.; Clerc, G.; Meibody-Tabar, F. Real-time detection of interturn faults in PM drives using back-EMF estimation and residual analysis. *IEEE Trans. Ind. Appl.* **2011**, *47*, 2402–2412. [[CrossRef](#)]
46. Sarikhani, A.; Mohammed, O.A. Inter-turn fault detection in PM synchronous machines by physics-based back electromotive force estimation. *IEEE Trans. Ind. Electron.* **2013**, *60*, 3472–3484. [[CrossRef](#)]
47. Guefack, F.L.T.; Kiselev, A.; Kuznetsov, A. Improved Detection of Inter-turn Short Circuit Faults in PMSM Drives using Principal Component Analysis. In Proceedings of the 2018 International Symposium on Power Electronics, Electrical Drives, Automation and Motion (SPEEDAM), Amalfi, Italy, 20–22 June 2018; pp. 154–159. [[CrossRef](#)]
48. Haddad, R.Z.; Strangas, E.G. On the Accuracy of Fault Detection and Separation in Permanent Magnet Synchronous Machines Using MCSA/MVSA and LDA. *IEEE Trans. Energy Convers.* **2016**, *31*, 924–934. [[CrossRef](#)]
49. Urresty, J.C.; Riba, J.R.; Romeral, L. Influence of the stator windings configuration in the currents and zero-sequence voltage harmonics in permanent magnet synchronous motors with demagnetization faults. *IEEE Trans. Magn.* **2013**, *49*, 4885–4893. [[CrossRef](#)]
50. Rosero, J.A.; Cusido, J.; Garcia, A.; Ortega, J.A.; Romeral, L. Study on permanent magnet demagnetization characteristics in permanent magnet synchronous machines. *Adv. Mater. Res.* **2011**, *211–212*, 127–131. [[CrossRef](#)]
51. Le Roux, W.; Harley, R.G.; Habetler, T.G. Detecting rotor faults in permanent magnet synchronous machines. In Proceedings of the 4th IEEE International Symposium on Diagnostics for Electric Machines, Power Electronics and Drives, 2003. SDEMPED 2003, Atlanta, GA, USA, 24–26 August 2003; Volume 22, pp. 198–203. [[CrossRef](#)]
52. Rajagopalan, S.; le Roux, W.; Habetler, T.G.; Harley, R.G. Dynamic eccentricity and demagnetized rotor magnet detection in trapezoidal flux (Brushless DC) motors operating under different load conditions. *IEEE Trans. Power Electron.* **2007**, *22*, 2061–2069. [[CrossRef](#)]
53. Faiz, J.; Mazaheri-Tehrani, E. Demagnetization Modeling and Fault Diagnosing Techniques in Permanent Magnet Machines under Stationary and Nonstationary Conditions: An Overview. *IEEE Trans. Ind. Appl.* **2017**, *53*, 2772–2785. [[CrossRef](#)]
54. Ding, S.; Hang, J.; Li, H.; Wang, Q. Demagnetisation fault detection in PMSM using zero sequence current components. *Electron. Lett.* **2017**, *53*, 148–150. [[CrossRef](#)]
55. Urresty, J.C.; Riba, J.R.; Delgado, M.; Romeral, L. Detection of demagnetization faults in surface-mounted permanent magnet synchronous motors by means of the zero-sequence voltage component. *IEEE Trans. Energy Convers.* **2012**, *27*, 42–51. [[CrossRef](#)]
56. Mohammed, A.; Melecio, J.I.; Durovic, S. Electrical Machine Permanent Magnets Health Monitoring and Diagnosis Using an Air-Gap Magnetic Sensor. *IEEE Sens. J.* **2020**, *20*, 5251–5259. [[CrossRef](#)]
57. Goktas, T.; Zafarani, M.; Lee, K.W.; Akin, B.; Sculley, T. Comprehensive Analysis of Magnet Defect Fault Monitoring Through Leakage Flux. *IEEE Trans. Magn.* **2017**, *53*, 8201010. [[CrossRef](#)]
58. Da, Y.; Shi, X.; Krishnamurthy, M. A new approach to fault diagnostics for permanent magnet synchronous machines using electromagnetic signature analysis. *IEEE Trans. Power Electron.* **2013**, *28*, 4104–4112. [[CrossRef](#)]

59. Ruschetti, C.R.; Verucchi, C.J.; Bossio, G.R.; García, G.O. A Model For Permanent Magnet Synchronous Machines With Demagnetization Faults. *IEEE Lat. Am. Trans.* **2013**, *11*, 414–420. [[CrossRef](#)]
60. Casadei, D.; Filippetti, F.; Rossi, C.; Stefani, A. Magnets Faults Characterization for Permanent Magnet Synchronous Motors. In Proceedings of the 2009 IEEE International Symposium on Diagnostics for Electric Machines, Power Electronics and Drives, Cargese, France, 31 August–3 September 2009; pp. 1–6.
61. Rosero, J.; Romeral, L.; Cusidó, J.; Ortega, J.A. Fault detection by means of wavelet transform in a PMSM under demagnetization. In Proceedings of the IECON 2007—33rd Annual Conference of the IEEE Industrial Electronics Society, Taipei, Taiwan, 5–8 November 2007; pp. 1149–1154. [[CrossRef](#)]
62. Riba Ruiz, J.R.; Rosero, J.A.; Garcia Espinosa, A.; Romeral, L. Detection of demagnetization faults in permanent-magnet synchronous motors under nonstationary conditions. *IEEE Trans. Magn.* **2009**, *45*, 2961–2969. [[CrossRef](#)]
63. Rosero, J.; Romeral, L.; Ortega, J.A.; Urresty, J.C. Demagnetization fault detection by means of hilbert huang transform of the stator current decomposition in PMSM. In Proceedings of the 2008 IEEE International Symposium on Industrial Electronics, Cambridge, UK, 30 June–2 July 2008; pp. 172–177. [[CrossRef](#)]
64. Espinosa, A.G.; Rosero, J.A.; Cusidó, J.; Romeral, L.; Ortega, J.A. Fault detection by means of Hilbert-Huang transform of the stator current in a PMSM with demagnetization. *IEEE Trans. Energy Convers.* **2010**, *25*, 312–318. [[CrossRef](#)]
65. Rajagopalan, S.; Restrepo, J.A.; Aller, J.M.; Habetler, T.G.; Harley, R.G. Detection of Rotor Faults in Brushless DC Motors Operating Under Nonstationary Conditions. *IEEE Trans. Ind. Appl.* **2006**, *42*, 1464–1477. [[CrossRef](#)]
66. Gritli, Y.; Rossi, C.; Casadei, D.; Zari, L.; Filippetti, F. Demagnetizations diagnosis for Permanent Magnet Synchronous Motors based on advanced Wavelet Analysis. In Proceedings of the 2012 20th International Conference on Electrical Machines, Marseille, France, 2–5 September 2012; pp. 2397–2403. [[CrossRef](#)]
67. Zhu, M.; Hu, W.; Kar, N.C. Torque-Ripple-Based Interior Permanent-Magnet Synchronous Machine Rotor Demagnetization Fault Detection and Current Regulation. *IEEE Trans. Ind. Appl.* **2017**, *53*, 2795–2804. [[CrossRef](#)]
68. Urresty, J.C.; Riba, J.R.; Romeral, L. A back-emf based method to detect magnet failures in PMSMs. *IEEE Trans. Magn.* **2013**, *49*, 591–598. [[CrossRef](#)]
69. Yang, Z.; Shi, X.; Krishnamurthy, M. Vibration monitoring of PM synchronous machine with partial demagnetization and inter-turn short circuit faults. In Proceedings of the 2014 IEEE Transportation Electrification Conference and Expo (ITEC), Dearborn, MI, USA, 15–18 June 2014. [[CrossRef](#)]
70. Ishikawa, T.; Seki, Y.; Kurita, N. Analysis for fault detection of vector-controlled permanent magnet synchronous motor with permanent magnet defect. *IEEE Trans. Magn.* **2013**, *49*, 2331–2334. [[CrossRef](#)]
71. Rajagopalan, S.; Restrepo, J.A.; Aller, J.M.; Habetler, T.G.; Harley, R.G. Wigner-Ville distributions for detection of rotor faults in brushless DC (BLDC) motors operating under non-stationary conditions. In Proceedings of the 2005 5th IEEE International Symposium on Diagnostics for Electric Machines, Power Electronics and Drives, Vienna, Austria, 7–9 September 2005; pp. 7–9. [[CrossRef](#)]
72. Delgado Prieto, M.; Garcia Espinosa, A.; Riba Ruiz, J.R.; Urresty, J.C.; Ortega, J.A. Feature Extraction of demagnetization faults in permanent-magnet synchronous motors based on box-counting fractal dimension. *IEEE Trans. Ind. Electron.* **2011**, *58*, 1594–1605. [[CrossRef](#)]
73. Ruiz, J.R.R.; Garcia Espinosa, A.; Romeral, L.; Cusidó, J. Demagnetization diagnosis in permanent magnet synchronous motors under non-stationary speed conditions. *Electr. Power Syst. Res.* **2010**, *80*, 1277–1285. [[CrossRef](#)]
74. Ebrahimi, B.M.; Faiz, J. Demagnetization fault diagnosis in surface mounted permanent magnet synchronous motors. *IEEE Trans. Magn.* **2013**, *49*, 1185–1192. [[CrossRef](#)]
75. Lee, K.W.; Hong, J.; Lee, S.B.; Lee, S. Quality assurance testing for magnetization quality assessment of BLDC motors used in compressors. *IEEE Trans. Ind. Appl.* **2010**, *46*, 2452–2458. [[CrossRef](#)]
76. Reigosa, D.; Fernandez, D.; Martinez, M.; Park, Y.; Lee, S.B.; Briz, F. Permanent Magnet Synchronous Machine Non-Uniform Demagnetization Detection Using Zero-Sequence Magnetic Field Density. *IEEE Trans. Ind. Appl.* **2019**, *55*, 3823–3833. [[CrossRef](#)]
77. Wang, C.; Delgado Prieto, M.; Romeral, L.; Chen, Z.; Blaabjerg, F.; Liu, X. Detection of Partial Demagnetization Fault in PMSMs Operating under Nonstationary Conditions. *IEEE Trans. Magn.* **2016**, *52*, 8105804. [[CrossRef](#)]
78. Guo, J.; Lu, S.; Zhai, C.; He, Q. Automatic bearing fault diagnosis of permanent magnet synchronous generators in wind turbines subjected to noise interference. *Meas. Sci. Technol.* **2018**, *29*, 025002. [[CrossRef](#)]
79. Picot, A.; Obeid, Z.; Regnier, J.; Maussion, P.; Poignant, S.; Darnis, O. Bearing fault detection in synchronous machine based on the statistical analysis of stator current. In Proceedings of the IECON 2012—38th Annual Conference on IEEE Industrial Electronics Society, Montreal, QC, Canada, 25–28 October 2012; pp. 3862–3867. [[CrossRef](#)]
80. Jankowska, K.; Ewert, P. Effectiveness Analysis of Rolling Bearing Fault Detectors Based On Self-Organising Kohonen Neural Network—A Case Study of PMSM Drive. *Power Electron. Drives* **2021**, *6*, 100–112. [[CrossRef](#)]
81. Ewert, P.; Orłowska-Kowalska, T.; Jankowska, K. Effectiveness analysis of pmsm motor rolling bearing fault detectors based on vibration analysis and shallow neural networks. *Energies* **2021**, *14*, 712. [[CrossRef](#)]
82. Rezig, A.; N'Diaye, A.; Mekideche, M.R.; Djerdir, A. Modelling and detection of bearing faults in Permanent Magnet Synchronous Motors. In Proceedings of the 2012 20th International Conference on Electrical Machines, Marseille, France, 2–5 September 2012; pp. 1778–1782. [[CrossRef](#)]

83. Wu, Z.; Niu, J.; Lu, S.; Liu, Y.; Liu, F. Fault Diagnosis of Wind Turbine Bearing Using Variational Nonlinear Chirp Mode Decomposition and Order Analysis. In Proceedings of the 2020 International Conference on Sensing, Measurement & Data Analytics in the era of Artificial Intelligence (ICSMD), Xi'an, China, 15–17 October 2020; pp. 479–484. [\[CrossRef\]](#)
84. Guo, J.; Wang, X.; Zhai, C.; Niu, J.; Lu, S. Fault diagnosis of wind turbine bearing using synchrosqueezing wavelet transform and order analysis. In Proceedings of the 2019 14th IEEE Conference on Industrial Electronics and Applications (ICIEA), Xi'an, China, 19–21 June 2019; pp. 2384–2387. [\[CrossRef\]](#)
85. Wang, X.; Niu, J.; Lu, S.; Liu, F.; Liu, Y. Improved Rotating Speed Estimation and Bearing Fault Diagnosis Using Multi-Channel Vibration Signals. In Proceedings of the 2020 International Conference on Sensing, Measurement & Data Analytics in the era of Artificial Intelligence (ICSMD), Xi'an, China, 15–17 October 2020; pp. 507–511. [\[CrossRef\]](#)
86. Rosero, J.; Romeral, J.L.; Cusido, J.; Ortega, J.A.; Garcia, A. Fault Detection of Eccentricity and Bearing Damage in a PMSM by means of Wavelet Transforms Decomposition of the Stator Current. In Proceedings of the 2008 Twenty-Third Annual IEEE Applied Power Electronics Conference and Exposition, Austin, TX, USA, 24–28 February 2008; pp. 111–116. [\[CrossRef\]](#)
87. Rosero, J.; Romeral, L.; Rosero, E.; Urresty, J. Fault detection in dynamic conditions by means of discrete wavelet decomposition for PMSM running under bearing damage. In Proceedings of the 2009 Twenty-Fourth Annual IEEE Applied Power Electronics Conference and Exposition, Washington, DC, USA, 15–19 February 2009; pp. 951–956. [\[CrossRef\]](#)
88. Gurusamy, V.; Baruti, K.H.; Zafarani, M.; Lee, W.; Akin, B. Effect of Magnets Asymmetry on Stray Magnetic Flux Based Bearing Damage Detection in PMSM. *IEEE Access* **2021**, *9*, 68849–68860. [\[CrossRef\]](#)
89. Mbo, C.P.; Hameyer, K. Fault diagnosis of bearing damage by means of the linear discriminant analysis of stator current features from the frequency selection. *IEEE Trans. Ind. Appl.* **2016**, *52*, 3861–3868. [\[CrossRef\]](#)
90. Mbo'O, C.P.; Hameyer, K. Bearing damage diagnosis by means of the linear discriminant analysis of stator current feature. In Proceedings of the 2015 IEEE 10th International Symposium on Diagnostics for Electrical Machines, Power Electronics and Drives (SDEMPED), Guarda, Portugal, 1–4 September 2015; pp. 296–302. [\[CrossRef\]](#)
91. Lee, J.S.; Yoon, T.M.; Lee, K.B. Bearing fault detection of IPMSMs using zoom FFT. *J. Electr. Eng. Technol.* **2016**, *11*, 1235–1241. [\[CrossRef\]](#)
92. Maliuk, A.S.; Prosvirin, A.E.; Ahmad, Z.; Kim, C.H. Novel Bearing Fault Diagnosis Using Gaussian Mixture Model-Based Fault Band Selection. *Sensors* **2021**, *21*, 6579. [\[CrossRef\]](#) [\[PubMed\]](#)
93. Wang, X.; Lu, S.; Huang, W.; Wang, Q.; Zhang, S.; Xia, M. Efficient Data Reduction at the Edge of Industrial Internet of Things for PMSM Bearing Fault Diagnosis. *IEEE Trans. Instrum. Meas.* **2021**, *70*, 3508612. [\[CrossRef\]](#)
94. Niu, J.; Lu, S.; Liu, Y.; Zhao, J.; Wang, Q. Intelligent bearing fault diagnosis based on tachless order tracking for a variable-speed AC electric machine. *IEEE Sens. J.* **2019**, *19*, 1850–1861. [\[CrossRef\]](#)
95. Lu, S.; He, Q.; Zhao, J. Bearing fault diagnosis of a permanent magnet synchronous motor via a fast and online order analysis method in an embedded system. *Mech. Syst. Signal Process.* **2018**, *113*, 36–49. [\[CrossRef\]](#)
96. Lu, S.; Wang, X.; He, Q.; Liu, F.; Liu, Y. Fault diagnosis of motor bearing with speed fluctuation via angular resampling of transient sound signals. *J. Sound Vib.* **2016**, *385*, 16–32. [\[CrossRef\]](#)
97. Yang, M.; Chai, N.; Liu, Z.; Ren, B.; Xu, D. Motor Speed Signature Analysis for Local Bearing Fault Detection with Noise Cancellation Based on Improved Drive Algorithm. *IEEE Trans. Ind. Electron.* **2020**, *67*, 4172–4182. [\[CrossRef\]](#)
98. Ren, B.; Yang, M.; Chai, N.; Li, Y.; Xu, D. Fault Diagnosis of Motor Bearing Based on Speed Signal Kurtosis Spectrum Analysis. In Proceedings of the 2019 22nd International Conference on Electrical Machines and Systems (ICEMS), Harbin, China, 11–14 August 2019. [\[CrossRef\]](#)
99. Ma, C.; Zuo, S. Black-box method of identification and diagnosis of abnormal noise sources of permanent magnet synchronous machines for electric vehicles. *IEEE Trans. Ind. Electron.* **2014**, *61*, 5538–5549. [\[CrossRef\]](#)
100. Frosini, L. Novel diagnostic techniques for rotating electrical machines—A review. *Energies* **2020**, *13*, 5066. [\[CrossRef\]](#)
101. Rifaq, M.S.; Lee, H.; Park, Y.; Lee, S.B.; Zapico, M.O.; Fernandez, D.; Diaz-Reigosa, D.; Briz, F. Airgap Search Coil Based Identification of PM Synchronous Motor Defects. *IEEE Trans. Ind. Electron.* **2022**, *69*, 6551–6560. [\[CrossRef\]](#)
102. Ebrahimi, B.M.; Faiz, J.; Roshtkhari, M.J. Static-, dynamic-, and mixed-eccentricity fault diagnoses in permanent-magnet synchronous motors. *IEEE Trans. Ind. Electron.* **2009**, *56*, 4727–4739. [\[CrossRef\]](#)
103. Goktas, T.; Zafarani, M.; Akin, B. Discernment of Broken Magnet and Static Eccentricity Faults in Permanent Magnet Synchronous Motors. *IEEE Trans. Energy Convers.* **2016**, *31*, 578–587. [\[CrossRef\]](#)
104. Koura, M.B.; Boudinar, A.H.; Aimer, A.F.; Bendiabdellah, A.; Gherabi, Z. Diagnosis and discernment between eccentricity and demagnetization faults in PMSM drives. *J. Power Electron.* **2021**, *21*, 563–573. [\[CrossRef\]](#)
105. Ahsanullah, K.; Jeyasankar, E.; Vignesh, A.N.; Panda, S.K.; Shanmukha, R.; Nadarajan, S. Eccentricity fault analysis in PMSM based marine propulsion motors. In Proceedings of the 2017 20th International Conference on Electrical Machines and Systems (ICEMS), Sydney, NSW, Australia, 11–14 August 2017. [\[CrossRef\]](#)
106. Akar, M.; Taşkın, S.; Şeker, S.; Cankaya, I. Detection of static eccentricity for permanent magnet synchronous motors using the coherence analysis. *Turk. J. Electr. Eng. Comput. Sci.* **2010**, *18*, 963–974. [\[CrossRef\]](#)
107. Galfarsoro, U.; McCloskey, A.; Hernandez, X.; Almandoz, G.; Zarate, S.; Arrasate, X. Eccentricity detection procedure in electric motors by force transducer and search coils in a novel experimental test bench. In Proceedings of the 2019 IEEE 12th International Symposium on Diagnostics for Electrical Machines, Power Electronics and Drives (SDEMPED), Toulouse, France, 27–30 August 2019; pp. 220–226. [\[CrossRef\]](#)

108. Kang, K.; Song, J.; Kang, C.; Sung, S.; Jang, G. Real-Time Detection of the Dynamic Eccentricity in Permanent-Magnet Synchronous Motors by Monitoring Speed and Back EMF Induced in an Additional Winding. *IEEE Trans. Ind. Electron.* **2017**, *64*, 7191–7200. [[CrossRef](#)]
109. Rosero García, J.; Romeral, J.L.; Rosero García, E. Detecting eccentricity faults in a PMSM in nonstationary conditions. *Ing. E Investig.* **2012**, *32*, 5–10.
110. Ilamparithi, T.; Nandi, S. Analysis, modeling and simulation of static eccentric reluctance synchronous motor. In Proceedings of the 8th IEEE Symposium on Diagnostics for Electrical Machines, Power Electronics & Drives, Bologna, Italy, 5–8 September 2011; pp. 45–50. [[CrossRef](#)]
111. Ilamparithi, T.C.; Nandi, S. Detection of eccentricity faults in three-phase reluctance synchronous motor. *IEEE Trans. Ind. Appl.* **2012**, *48*, 1307–1317. [[CrossRef](#)]
112. Pazouki, E.; Islam, M.Z.; Bonthu, S.S.R.; Choi, S. Eccentricity fault detection in multiphase permanent magnet assisted synchronous reluctance motor. In Proceedings of the 2015 IEEE International Electric Machines & Drives Conference (IEMDC), Coeur d’Alene, ID, USA, 10–13 May 2015; pp. 240–246. [[CrossRef](#)]
113. Mahmoud, H.; Bianchi, N. Eccentricity in Synchronous Reluctance Motors—Part II: Different Rotor Geometry and Stator Windings. *IEEE Trans. Energy Convers.* **2015**, *30*, 754–760. [[CrossRef](#)]
114. López-Torres, C.; Riba, J.R.; García, A.; Romeral, L. Detection of eccentricity faults in five-phase ferrite-PM assisted synchronous reluctance machines. *Appl. Sci.* **2017**, *7*, 565. [[CrossRef](#)]
115. Gherabi, Z.; Benouzza, N.; Toumi, D.; Bendiabdellah, A. Eccentricity Fault diagnosis in PMSM using Motor Current Signature Analysis. In Proceedings of the 2019 International Aegean Conference on Electrical Machines and Power Electronics (ACEMP) & 2019 International Conference on Optimization of Electrical and Electronic Equipment (OPTIM), Istanbul, Turkey, 27–29 August 2019; pp. 205–210. [[CrossRef](#)]
116. Karami, M.; Mariun, N.; Mehrjou, M.R.; Ab Kadir, M.Z.A.; Misron, N.; Mohd Radzi, M.A. Static Eccentricity Fault Recognition in Three-Phase Line Start Permanent Magnet Synchronous Motor Using Finite Element Method. *Math. Probl. Eng.* **2014**, *2014*, 132647. [[CrossRef](#)]
117. Ebrahimi, B.M.; Faiz, J. Configuration impacts on eccentricity fault detection in permanent magnet synchronous motors. *IEEE Trans. Magn.* **2012**, *48*, 903–906. [[CrossRef](#)]
118. Ebrahimi, B.M.; Roshtkhari, M.J.; Faiz, J.; Khatami, S.V. Advanced Eccentricity Fault Recognition in Permanent Magnet Synchronous Motors Using Stator Current Signature Analysis. *IEEE Trans. Ind. Electron.* **2014**, *61*, 2041–2052. [[CrossRef](#)]
119. Lin, F.; Zuo, S.; Deng, W. Impact of rotor eccentricity on electromagnetic vibration and noise of permanent magnet synchronous motor. *J. Vibroengineering* **2018**, *20*, 923–935. [[CrossRef](#)]
120. Galfarsoro, U.; McCloskey, A.; Zarate, S.; Hernández, X.; Almandoz, G. Influence of Manufacturing Tolerances and Eccentricities on the Electromotive Force in Permanent Magnet Synchronous Motors. In Proceedings of the 2022 International Conference on Electrical Machines (ICEM), Valencia, Spain, 5–8 September 2022; pp. 703–709. [[CrossRef](#)]
121. Hong, J.; Park, S.; Hyun, D.; Kang, T.J.; Lee, S.B.; Kral, C.; Haumer, A. Detection and classification of rotor demagnetization and eccentricity faults for PM synchronous motors. *IEEE Trans. Ind. Appl.* **2012**, *48*, 923–932. [[CrossRef](#)]
122. Hong, J.; Lee, S.B.; Kral, C.; Haumer, A. Detection of airgap eccentricity for permanent magnet synchronous motors based on the d-axis inductance. *IEEE Trans. Power Electron.* **2012**, *27*, 2605–2612. [[CrossRef](#)]
123. Park, Y.; Yang, C.; Lee, S.B.; Lee, D.M.; Fernandez, D.; Reigosa, D.; Briz, F. Online detection and classification of rotor and load defects in PMSMs Based on Hall sensor measurements. *IEEE Trans. Ind. Appl.* **2019**, *55*, 3803–3812. [[CrossRef](#)]
124. Ewert, P.; Jaworski, M. Application of selected higher-order methods to detect rotor unbalance of drive system with PMSM. In Proceedings of the 2021 IEEE 19th International Power Electronics and Motion Control Conference (PEMC), Gliwice, Poland, 25–29 April 2021; pp. 874–879. [[CrossRef](#)]
125. Hang, J.; Zhang, J.; Cheng, M.; Wang, Z. Fault diagnosis of mechanical unbalance for permanent magnet synchronous motor drive system under nonstationary condition. In Proceedings of the 2013 IEEE Energy Conversion Congress and Exposition, Denver, CO, USA, 15–19 September 2013; pp. 3556–3562. [[CrossRef](#)]
126. Rifaq, M.S.; Lee, H.; Park, Y.; Lee, S.B.; Fernandez, D.; Diaz-Reigosa, D.; Briz, F. A Simple Method for Identifying Mass Unbalance Using Vibration Measurement in Permanent Magnet Synchronous Motors. *IEEE Trans. Ind. Electron.* **2022**, *69*, 6441–6444. [[CrossRef](#)]
127. Park, C.H.; Lee, J.; Ahn, G.; Youn, M.; Youn, B.D. Fault Detection of PMSM under Non-Stationary Conditions Based on Wavelet Transformation Combined with Distance Approach. In Proceedings of the 2019 IEEE 12th International Symposium on Diagnostics for Electrical Machines, Power Electronics and Drives (SDEMPED), Toulouse, France, 27–30 August 2019; pp. 88–93. [[CrossRef](#)]
128. Huang, X.; Yang, M.; Ren, B.; Chai, N.; Xu, D. Angle misalignment detection and its suppression algorithm in rotor system based on speed signal. In Proceedings of the 2020 IEEE 9th International Power Electronics and Motion Control Conference (IPEMC 2020 ECCE Asia), Nanjing, China, 29 November–2 December 2020; pp. 3174–3179. [[CrossRef](#)]
129. Chai, N.; Yang, M.; Ren, B.; Huang, X.; Xu, D. Misalignment Detection of Rotor System Based on Adaptive Input-output Model Identification of Motor Speed. In Proceedings of the 2020 IEEE 9th International Power Electronics and Motion Control Conference (IPEMC 2020 ECCE Asia), Nanjing, China, 29 November–2 December 2020; pp. 2266–2271. [[CrossRef](#)]
130. Pietrzak, P.; Wolkiewicz, M. Application of Spectral and Wavelet Analysis of Stator Current to Detect Angular Misalignment in PMSM Drive Systems. *Power Electron. Drives* **2021**, *6*, 42–60. [[CrossRef](#)]

131. Zamudio-Ramirez, I.; Ramirez-Nunez, J.A.; Antonino-Daviu, J.; Osornio-Rios, R.A.; Quijano-Lopez, A.; Razik, H.; De Jesus Romero-Troncoso, R. Automatic Diagnosis of Electromechanical Faults in Induction Motors Based on the Transient Analysis of the Stray Flux via MUSIC Methods. *IEEE Trans. Ind. Appl.* **2020**, *56*, 3604–3613. [[CrossRef](#)]
132. Liu, X.; Liang, D.; Du, J.; Yu, Y.; Yang, X.; Luo, Z. Effects analysis of misalignments on dynamic characteristics test for permanent magnet synchronous motor. In Proceedings of the 2014 17th International Conference on Electrical Machines and Systems (ICEMS), Hangzhou, China, 22–25 October 2014; pp. 1543–1547. [[CrossRef](#)]
133. Yao, Y.; Li, Y.; Yin, Q. A novel method based on self-sensing motor drive system for misalignment detection. *Mech. Syst. Signal Process.* **2019**, *116*, 217–229. [[CrossRef](#)]
134. Wikimedia. 2013. Available online: [https://commons.wikimedia.org/wiki/File:Pump\\_diagram.PNG](https://commons.wikimedia.org/wiki/File:Pump_diagram.PNG) (accessed on 12 November 2013).

**Disclaimer/Publisher’s Note:** The statements, opinions and data contained in all publications are solely those of the individual author(s) and contributor(s) and not of MDPI and/or the editor(s). MDPI and/or the editor(s) disclaim responsibility for any injury to people or property resulting from any ideas, methods, instructions or products referred to in the content.